«ФИЗИКА ЭЛЕМЕНТАРНЫХ ЧАСТИЦ И АТОМНОГО ЯДРА»
1996, ТОМ 27, ВЫП.6

УДК 539.12.01
539.14.141

NEUTRAL CURRENTS IN LOW ENERGY NUCLEAR PHYSICS PROCESSES

O. Dumitrescu

International Centre for Theoretical Physics, Trieste, Italy
and
Department of Theoretical Physics, Institute of Physics and Nuclear Engineering,
Institute of Atomic Physics
Magurele, P.O.Box MG–6, R–76900, Bucharest, Romania

The possibility of extracting from the experiment the necessary information concerning the neutral current contributions to the structure of the weak interactions that violate the parity conservation law is investigated. The parity nonconservation (PNC) induced by weak hadron-hadron interactions investigated via low energy nuclear physics processes is reviewed. The low energy nuclear physics processes considered here are: the resonance nuclear scattering and reactions induced by polarized projectiles such as protons and deuterons, emission of polarized gamma rays from oriented and nonoriented nuclei and parity forbidden alpha decays. Some comments on PNC nucleon-nucleon (PNCNN) interaction are presented. Explicit expressions for some PNC observables are rederived. Applications for specific scattering, reaction and decay modes are done. New experiments are proposed.

Исследуется возможность извлечения из эксперимента информации о вкладе нейтральных токов в слабые взаимодействия, приводящем к нарушению четности. В обзоре рассматривается нарушение четности (НЧ), индуцированное слабым адрон-адронным взаимодействием и исследуемое в низкоэнергетических ядерных процессах. Рассматриваются такие процессы, как резонансное ядерное рассеяние, реакции, индуцированные поляризованными частицами (протоны и дейтроны), гамма-излучение ориентированных и неориентированных ядер, запрещенный по четности альфа-распад. Обсуждается нарушающее четность нуклон-нуклонное (НЧНН) взаимодействие. Заново получены точные выражения для некоторых наблюдаемых в НЧ процессах. Даны приложения для ряда специфических случаев рассеяния, реакций и распада. Предлагаются новые эксперименты.

1. INTRODUCTION

The existence of the neutral currents other than the familiar electromagnetic currents was predicted as early as 1958 by Bludman [1], who constructed a model based on a local SU(2) gauge symmetry. This model incorporated both

the charged (entering the β-decay interaction) and neutral currents. The space-time structure of the neutral currents in this first model was of a pure vector minus axial vector (V–A) type. Thus they could not be identified with the electromagnetic currents which are of a pure vectorial and parity conserving type. There was no unification with the electromagnetism in Bludman's model. A model truly unifying weak and electromagnetic interactions incorporating two kinds of neutral currents (electromagnetic and weak) was invented by Glashow [2] and by Salam and Ward [3]. This model is the SU(2) ⊗ U(1) model. As is stated in this last model, there is no mechanism for the mass generation of the intermediate vector bosons. Thus the relative strength of weak neutral-current interactions to that of charged-current interactions is a completely free parameter. This problem was settled by Weinberg [4], who incorporated the idea of spontaneous breakdown of local gauge symmetry [5], [6], into the SU(2) ⊗ U(1) model. An analogous mechanism was proposed by Salam [7]. The mass of the intermediate boson (Z) that mediates the neutral current is related in a definite way to the mass of its charged counterpart (W). The above relative strength was therefore fixed once and for all, in this version of the SU(2) ⊗ U(1) model, predicting in this way the structure of the weak neutral currents (as a mixture of vector and axial vector currents) and its strength of interaction. Thus the SU(2) ⊗ U(1) model became a single parameter ($\sin^2 \theta_W$) theory. With the discovery of neutral currents in 1973 [8], this standard SU(2) ⊗ U(1) field theory, stood out as a strong candidate for a unique theory of electroweak interactions. In the following years a great progress has been made in understanding the weak NN interactions, especially after the experimental detection [9], [10] of $W^{\pm}$ and Z^0 bosons, mediators of the weak force.

The weak interactions between the nucleons and especially those components with dominant contribution of the neutral currents can be studied only when the strong and electromagnetic interactions between the nucleons are forbidden by a symmetry principle, such as flavor (i.e., strangeness (S) or charm (C)) conservation. According to the standard theory, the neutral current contributions to $\Delta S = 1$ and $\Delta C = 1$ weak processes are strongly suppressed [11], [12] and, therefore, the neutral-current weak interaction between quarks can only be studied in flavor conserving processes which can be met in the low energy nuclear physics processes. The isovector part of the charged current weak interaction is suppressed by $\tan^2 \theta_C$ [11], [12], where θ_C is the Cabbibo angle, therefore the isovector part of the weak interaction contains mainly the neutral currents. Thus, the PNC nuclear physics processes determined by an isovector PMD are very important for the studies of the neutral currents.

The search for parity nonconservation (PNC) in complex nuclei, and especially in cases where an enhanced effect is expected from the existence of parity mixed doublets (PMD) [13–41] has a long history. The enhancement of any PNC effect is predicted by several reasons, the most important being the small level spacing between states of the same spin and opposite parity in the compound nucleus involved. The second one arises from the expected increase of the ratio (f) between parity-forbidden and parity-allowed transition matrix elements caused by the nuclear structure of the states involved. Usually such enhancements are offset due to correspondingly large theoretical uncertainties in the extraction of the PNC-NN parameters from the experimental data. As a matter of fact the same conditions which generate the enhancement complicate a reliable determination of the nuclear matrix elements theoretically. Therefore, it is necessary to select exceptional cases, in which the nuclear structure problem can be solved. This is the case for closely spaced doublets of the same spin and opposite parity levels situated far away from other similar levels. In this case the parity impurities are well approximated by simple two state mixing, which simplifies the analysis and isolates specific components of the PNC-NN interaction. Bearing in mind that for PMD's the ratio $\frac{M_{PNC}}{\Delta E}$ (which estimates roughly the corresponding PNC effect) usually is of the order of 10^{-8} for $\Delta E \geq 1.0$ MeV we can define a specific enhancement factor: $F = 10^8 \cdot \frac{M_{PNC}}{\Delta E} \cdot f$, where f is a ratio of the decay (formation) amplitude corresponding to the small lifetime (large width) level to that of the large lifetime (small width) level.

The effects related to the PMD should help to determine the relative strengths of the different components of the PNC nucleon-nucleon (PNC-NN) interaction [13], [16], [14], [15]. Due to the generally small values of most of the contributing terms to the PNC matrix elements, PNC dealing with low energy nuclear spectrum should essentially involve the strength of the nucleon-nucleus weak force. As weak interactions do not conserve the isospin, this strength may be characterized by two numbers, relative to the proton and neutron forces, respectively, or equivalently to its isovector and isoscalar components. Moreover, the main contribution coming from the isovector part is assumed to be due to the one pion exchange term (the long range term), while the main contribution coming from the isoscalar part is assumed to be due to one ρ-meson exchange term (the short range term). At present no experiment is possible to invent in order to be sensible to other contributions to the weak hadron-hadron interaction potential. Therefore, in principle, two independent experiments should be sufficient for the determination of the above nucleon-

nucleus weak forces. They may be those looked at in ^{19}F, whose theoretical analysis [24], [25], [16] shows it is dominated by the strength of the proton-nucleus weak force [23], and in ^{18}F, which is well known to be dominated by the isovector part of this force. The firs effect, experimentally observed [18], [19], is accounted for by the «*best DDH values*» [13] of meson-nucleon weak coupling constants. The second one is not, although it is compatible with the largest range of their expectations. Several cases have been proposed theoretically, but only few of them have been experimentally investigated; only the ^{18}F experiments (average of 5 investigations [49], [50], [51], [52], [53]) [16] gives a reliable upper limit (i.e., $\simeq 10^{-7}$) for the weak pion-nucleon coupling constant. The result is not in contradiction to the predictions of Refs.[13], [14], [15], especially, if taking into account the more sophisticated recent shell model calculations [29], [43], which indicate values for the circular polarization much smaller than $\simeq 10^{-4}$. In addition, if one takes into account the analyzing power ($\simeq 2 \cdot 10^{-2}$) [17] of the Compton polarimeters, this would require a precision $\simeq 1.2 \cdot 10^{-5}$ in the counting asymmetry and that it might be very difficult to maintain the systematic errors lower than this limit. Therefore, additional investigations are necessary, especially with independent observables.

This goal was a challenge in the past 15 years. Several pairs of experiments have been proposed in order to separate the isoscalar contributions of the PNC weak force from the isovector ones. Among them we mention the cases presented in Table 1.

Table 1. Several parity mixed doublets

Nucleus	$J_1^\pi T_1$	$J_2^\pi T_2$	E_1 (MeV)	E_2 (MeV)	Γ_1 (keV)	Γ_2 (keV)	f	V (eV)	F (10^3)	Q_{exp} (10^{-5})	Refs.
^{10}B	2^-0	2^+1	5.1103	5.1639	1.2	0.002	24.4	0.1	4.6		[17]
^{13}N	$\frac{3^-}{2}$	$\frac{3^+}{2}$	15.065	14.05	0.86	165	14	0.9	$\simeq 1$		
^{13}N	$\frac{5^-}{2}$	$\frac{5^+}{2}$	11.7	11.53	115	430	1.7	0.9	$\simeq 1$		
^{14}N	0^-1	0^+1	8.796	8.624	410	3.8	10.4	1.04	6.3	0.86	[56], [16]
^{14}N	2^-0	2^+1	9.3893	9.17225	13	0.135	9.8	0.5	2.5		[38]
^{14}N	(2^-)	(2^+)	11.67	11.51	150	7	4.6	0.5	1.5		

Nucleus	$J_1^{\pi}T_1$	$J_2^{\pi}T_2$	E_1 (MeV)	E_2 (MeV)	Γ_1 (keV)	Γ_2 (keV)	f	V (eV)	F (10^3)	Q_{exp} (10^{-5})	Refs.
^{15}O	$\frac{3}{2}^-$	$\left(\frac{3}{2}\right)^+$	9.609	9.527	8.8	280	5.6	0.2	$\simeq 1.5$		
^{15}N	$\frac{1}{2}^-$	$\frac{1}{2}^+$	11.2928	11.437	8	41.4	2.3	0.8	$\simeq 1.3$		
^{16}O	2^-1	2^+0	12.9686	13.020	1.6	150	9.7	0.1	1.9		[34]
^{16}O	1^+1	1^-0	16.209	16.20	19	580	5.5	0.1	2.5		[42]
^{17}O	$\frac{1}{2}^-$	$\frac{1}{2}^+$	6.862	6.356	≤ 1	124	≥ 11	0.6	$\simeq 1$		
^{17}O	$\frac{1}{2}^-$	$\frac{1}{2}^+$	7.99	7.956	270	90	1.73	0.3	$\simeq 1.5$		
^{18}F	0^-0	0^+1	1.08054	1.04155	27.5 ps	2.55 fs	112	0.37	103	80	[16]
^{18}F	2^-	2^+	6.809	6.811	88	3	5.4	0.5	130		
^{19}F	$\frac{1}{2}^-\frac{1}{2}$	$\frac{1}{2}^+\frac{1}{2}$	0.109844	0.0	0.85 ns		11	0.46	4.6	-7.1	[16]
^{19}F	$\frac{3}{2}^-\frac{1}{2}$	$\frac{3}{2}^+\frac{1}{2}$	1.4587	1.554	90	5	4.3	0.4	1.7		
^{20}Ne	1^-0	1^+1	11.240	11.2623	175		≥ 1	$\simeq 0.5$	≥ 2.5		
^{20}Ne	2^-1	2^+0	11.601	11.885		46	≥ 1	$\simeq 0.8$	≥ 0.8		
^{20}Ne	1^-0	1^+1	13.461	13.484	195	6.4	5.5	0.2	5	150	[31]
^{21}Ne	$\frac{1}{2}^+\frac{1}{2}$	$\frac{1}{2}^-\frac{1}{2}$	2.795	2.789	7.6 fs	117 ps	296	0.006	29.6	0.8	[16]
^{23}Na	$\frac{5}{2}^+\frac{1}{2}$	$\frac{5}{2}^-\frac{1}{2}$	3.9147	3.818	8 fs	90 fs	6.8	0.3	3.0		[30]
^{30}P	2^+1	2^-0	4.1826	4.1436	3.2 fs	42 fs	14	1.0	36		[30]
^{30}P	2^+1	2^-1	7.284	7.224		4.5	≥ 1	$\simeq 0.1$	≥ 0.2		
^{30}Si	2^+1	2^-0	6.537	6.6414	≤ 25 fs	33 fs	≥ 1.15	0.8	$\simeq 1$		
^{36}Cl	2^+1	2^-1	1.95921	1.95105	60 fs	2.6 ps	6.6	≥ 0.1	≥ 8		[46]
^{36}Ar	2^+	2^-	4.9512	4.974	≤ 50 fs	14 ps	≥ 16	≥ 0.1	≥ 8		[46]

Nucleus	$J_1^{\pi}T_1$	$J_2^{\pi}T_2$	E_1 (MeV)	E_2 (MeV)	Γ_1 (keV)	Γ_2 (keV)	f	V (eV)	F (10^3)	Q_{exp} (10^{-5})	Refs.
^{180}Hf	8^-	8^+	1.14161	1.08407	5.5 h	2.18 ps	10^7(*)	$\simeq 10^{-5}$	10^3	− 1660	[124]
^{223}Th	$\frac{13^-}{2}$	$\frac{13^+}{2}$	0.324	0.320			1.7	$\simeq 0.5$	≥ 21.5		[125]

Several studied parity mixed doublets [30]. E_i and Γ_i stand for the excitation energies and total widths of the PMD levels, f — the «small enhancement factor is due to the parity conserving sector, while F — the «big» enhancement factor incorporates the PNC matrix element (M_{PNC}) also and Q_{exp} stands for the measured pseudoscalar observable (analyzing power, circular polarization or gamma asymmetry as explained in the cited references). All the experimental data are taken from Refs.[64] or [132] except those for ^{180}Hf and ^{223}Th, which are taken from Refs. [131] and [125], respectively. The estimations for the PNC matrix elements, if not specified, are performed within OXBASH-code [63]. Exact calculations are not possible in some cases because the isospins and sometimes the spins of some lower lying states are not known or the OXBASH-code has not quite good interactions for those cases. In the ^{36}Cl and ^{36}Ar cases, within the D3F7 model space (see Ref.[46]), the single particle contributions to the total PNC matrix elements vanish. Within a larger model space, these contributions are included and such calculations show larger PNC matrix elements (see section 5.4).

(*) The branching ratios (ratio between the partial and the total gamma widths) $b_- = 0.1564$ for $M2 + E3$ transition (the sign «–» stands for the parity «–» level of the PMD) and $b_+ = 0.855$ for $E2$ transition (the sign «+» stands for the parity «+» level of the PMD) are taken from [131].

The above selection could be reasonable due to the fact that the shell structure problems, for one nucleus or two adjacent mirror nuclei in selecting the relative weight of the isovector and isoscalar terms entering the structure of the PNC weak force, should not be too different. Unfortunately, the lack of such *«pair»* experimental data does not allow us to extract with high accuracy the isovector and isoscalar components directly from the experiment.

Investigating the PNC meson-nucleon vertices within the framework of a chiral effective Lagrangian for π, ρ and ω meson exchange and treating nucleons as topological solitons, the weak πN coupling constant (h_π) is found [15] to be considerably smaller ($(2.0)\cdot 10^{-8}$) than the standard quark model results ($(1.3)\cdot 10^{-7}$) [14], both restricting the often used Desplanques, Donoghue, Holstein (DDH)-values [13] significantly. Such a controversy stimulates us to investigate experiments sensitive to h_π with large interest.

2. NATURE OF THE HADRON-HADRON WEAK INTERACTION THAT VIOLATES THE PARITY CONSERVATION LAW

In 1957, the same year that PNC was discovered in β and μ decay, Tanner [79] reported the first research concerning the parity violation in the hadron-hadron interaction, namely the parity forbidden α-decay of ^{20}Ne (^{20}Ne($J^{\pi}T = 1^{+}0$, $E_x = 13.19$ MeV) $\rightarrow {}^{16}\mathrm{O} + \alpha_0$). Then it followed the Feynmann–Gell-Mann [80] universal current-current theory of weak interactions, in which it is predicted, in addition to the known weak processes of β, μ and hyperon decay, a weak parity violating interaction between the nucleons, experimentally established by Lobashev and his co-workers [81], [66].

According to the standard SU(2) ⊗ U(1) theory of electroweak interactions and quantum chromodynamics (QCD), the nuclear PNC effects arise through the weak emission and absorption of the gauge bosons $W^{\pm}$ and Z^0 by the quarks in the hadrons. Actually, due to the large masses of the gauge bosons, this elementary weak interaction is of extremely short range. On the other hand, at low energies the nucleons are prevented from coming close together, owing to the hard core in the strong nucleon-nucleon potential. A gauge boson emitted by a quark is subsequently absorbed by a quark belonging to the same nucleon. Therefore, the exchange of a gauge boson between distinct nucleons is a highly improbable process. As a result, the nucleon passes into an excited state of quarks, which, at low energies, can be reasonably assumed to be a meson-nucleon state. The meson appears to be emitted by the nucleon through a weak PNC process, with an effective coupling constant which includes all the elementary weak ($h^{(\Delta T)}_{\mathrm{meson}}$) and strong ($g^{(\Delta T)}_{\mathrm{meson}}$) interactions of the quarks contributed to the emission. PNC process in nuclei arises, therefore, through a weak PNC emissions and absorption of low-mass mesons (π, ρ, and ω) by the nucleons inside the nucleus, neutral scalar mesons being excluded by CP conservation [16,17,82].

The magnitude of the weak interaction can be estimated, e.g., from the charged weak Hamiltonian [17]:

$$H_W = g^2 \int d^3x_1 d^3x_2 \, j^{\mu}(x_1) \, e^{\frac{-M_W r_{12}}{r_{12}}} \, j^{\dagger}_{\mu}(x_2). \tag{1}$$

The mass of the W- boson is very large, and the associated length very short, at the nuclear scale: $M_W \simeq 80$ GeV, $M_W^{-1} \simeq 2 \cdot 10^{-3}$ fm, [9], [10]. One can, therefore, approximate $e^{\frac{-M_W r_{12}}{r_{12}}}$ with a δ-function, and the above equation (1) gives

$$H_W = \frac{G}{\sqrt{2}} \int d^3x_1 d^3x_2 j^{\mu}(x_1) j_{\mu}^{\dagger}(x_2) \tag{2}$$

with $G = 4\pi\sqrt{2}q^2/M_W$, thus the weak coupling constant is of the order of $h \approx g/M_W$.

In the low energy regime of interest to us, the hadronic weak interaction can be described by a phenomenological current-current Lagrangian [92], [93]

$$L = \frac{G_F}{\sqrt{2}} \left(J_C^{\dagger} J_C + 2 \left(\frac{M_W}{M_Z \cos\theta_C} \right)^2 J_N^{\dagger} J_N + \text{h.c.} \right), \tag{3}$$

where J_C and J_N are the charged and neutral currents, respectively and

$$\frac{G_F}{\sqrt{2}} = \frac{\pi\alpha}{2M_W^2 \sin^2\theta_W}, \tag{4}$$

where $\alpha = e^2/4\pi$ is the fine structure constant, M_W and M_Z are the masses of the heavy $W^{\pm}$ and Z bosons, respectively, while θ_C and θ_W are the Cabbibo and Weinberg angles, respectively.

The charged current J_C has two components:

$$J_C = \cos\theta_C J_W^0 + \sin\theta_C J_W^1. \tag{5}$$

The superscripts 0 and 1 stand for the amount of the isospin transfer (ΔT). The neutral current J_Z also has two components, J_Z^0 and J_Z^1, which transform as $\Delta T = 0$ and 1, respectively. All the components of the charge and neutral currents, except the J_W^1 component of the charge current, transform as $\Delta S = 0$, where S is the strangeness quantum number. The component J_W^1 is not very important because it is suppressed by $\tan^2\theta_C$ [11], [12]. On the other hand, the $\Delta T = 1$ neutral current contribution is not suppressed. Therefore, on these simple grounds, we expect the neutral current to dominate the $\Delta T = 1$ PNC nucleon-nucleon interaction. However, the strong interaction can significantly alter the PNC matrix elements, so this qualitative isospin argument may not be always valid.

The earliest experiments [8] have used the knowledge of low-energy nuclear interactions and looked for the very small ($\approx 10^{-6}$) parity-mixing of levels at the magnitude expected on the basis of previous studies in the language of meson exchange [94].

It is well known that the parity conserving (PC) nucleon-nucleon force can be described reasonably well in terms of a coherent superpositions of diagrams for meson exchange. In a similar fashion one generally represents the PNC-NN potential in terms of a sum of diagrams involving exchange of a single meson between pairs of nucleons. There is an important difference in this case, however, in that one meson-nucleon vertex is weak and one is strong. As far as CP violation is negligible [82], the PNC-NN potential is determined by π, ρ, and ω exchange.

Since the strong coupling constants are empirically known, one finds a form of the PNC-NN potential in terms of seven weak coupling constants ($h^{\Delta T}_{\text{meson}}$). All the physics of W and Z exchange between the quarks of the nucleons and mesons is hidden inside of these weak coupling constants [13], [14], [15], [95]. The shape of this PNC interaction potential is determined by the nature of the exchanged meson.

Coming back to the approaches to get a handle on the weak coupling constants ($h^{\Delta T}_{\text{meson}}$) some comments could be in order here.

Within the standard model, one needs to calculate the weak meson-nucleon vertices. Only a few calculations based on the quark model [13], [14], [58], [59], [61], [62] exist. In Refs. [13,14] the authors employed a SU(6) quark model to calculate six weak meson-nucleon coupling constants ($h^{\Delta T}_{\text{meson}}$), denoted: $h^{(1)}_{\pi}$, $h^{(0)}_{\rho}$, $h^{(1)}_{\rho}$, $h^{(2)}_{\rho}$, $h^{(0)}_{\omega}$, $h^{(1)}_{\omega}$. These calculations start from the observation that there are essentially three types of diagrams, which can be categorized as factorization, quark-model and sum-rule contributions. Renormalization group techniques and baryon wave functions based on phenomenological models are needed to evaluate them. This introduces a variety of uncertainties ($\cong 300\%$), which lead DDH in Ref. [13] to introduce a «reasonable range» for the values of the weak meson-nucleon coupling constants. In particular the weak pion-nucleon coupling constant (h_{π}) is very sensitive with respect to these uncertainties, for instance, the values of h_{π} differ by a factor of 3 in Refs.[13] and [14], whereas $h_{\rho(\omega)}$ are more stable. In addition, recent QCD sum rule applications lead [59] to the estimate $h^{(1)}_{\pi} \approx (3.0)\cdot 10^{-8}$. QCD sum rules have been shown to be able to reproduce known properties of the nucleon, e.g., μ_p, μ_n, g_A and of other hadrons [60]. However, they have rarely (if ever) been used to predict unknown properties, such like the value of $h^{(1)}_{\pi}$.

By using a nonlinear chiral effective Lagrangian which includes π, ρ, and ω mesons and treating nucleons as topological solitons Kaiser and Meissner

[15] obtained slightly different values for strong and weak meson-nucleon coupling constants as compared to the results from Refs. [13], [14]. The largest discrepancy conserns the weak meson-nucleon vertex coupling constant — h_π, which is 20 times smaller than the «best value» given in Ref.[13]. Moreover Kaiser and Meissner [15] obtained in addition the 7th weak meson-nucleon vertex coupling constant — $(h^{(1)}_{\rho'})$ with a quite large value, giving a comparable contribution to the pion term in some PNC processes (see for example Refs.[46], [47]). For comparison we inserted in the calculations of the PNC matrix element above mentioned the coupling constants of the weak meson-nucleon vertices h_π, h_ρ, and h_ω calculated within different models of weak interactions and summarized in Tables 2 and 3. The first column of Table 2 contains $h^{(\Delta T)}_m$ obtained by Kaiser and Meissner (KM) [15] using his model parameters as follows: the pion decay constant $f_\pi = 93$ MeV, the «gauge» coupling constant $g_{\rho\pi\pi} = 6$, the pion mass $m_\pi = 138$ MeV and three pseudo-scalar-vector coupling constants (see Table 1 of Ref.[15], Table 2 of the same Ref.[15] includes the

Table 2

$h^{(\Delta T)}_{\text{meson}}$	KM	DDH	AH (fit)	DZ
$h^{(1)}_\pi$	0.19	4.54	2.09	1.30
$h^{(0)}_\rho$	− 3.70	− 11.40	− 5.77	− 8.30
$h^{(1)}_\rho$	− 0.10	− 0.19	− 0.22	0.39
$h^{(2)}_\rho$	− 3.30	− 9.50	− 7.06	− 6.70
$h^{(1)}_{\rho'}$	− 2.20	0.00	0.00	0.00
$h^{(0)}_\omega$	− 1.40	− 1.90	− 4.97	− 3.90
$h^{(1)}_\omega$	− 1.00	− 1.10	− 2.39	− 2.20

Weak meson-nucleon coupling constants calculated within different weak interaction models (in units of 10^{-7}). The abbreviations are: KM — Kaiser and Meissner [15], DDH — Desplanques, Donoghue and Holstein «best» values [13], AH — Adelberger and Haxton [16] and DZ — Dubovik and Zenkin [14].

Table 3

$F^{(\Delta T)}_{k,s}$	KM	DDH
$F^{(1)}_{0,\pi} = \frac{1}{2\sqrt{2}} g_\pi h^{(1)}_\pi$	0.090	2.16
$F^{(1)}_{1,\rho} = -\frac{1}{2} g_\rho h^{(1)}_\rho$	0.014	0.027
$F^{(1)}_{2,\rho} = -\frac{1}{2} g_\rho h^{(1)}_\rho (1+\mu_v)$	0.066	0.127
$F^{(1)}_{3,\rho} = \frac{1}{2} g_\rho h^{(1)}_\rho$	− 0.014	− 0.027
$F^{(1)}_{1,\omega} = -\frac{1}{2} g_\omega h^{(1)}_\omega$	0.437	0.480
$F^{(1)}_{2,\omega} = -\frac{1}{2} g_\omega h^{(1)}_\omega (1+\mu_s)$	0.384	0.423
$F^{(1)}_{3,\omega} = -\frac{1}{2} g_\omega h^{(1)}_\omega$	0.437	0.480
$F^{(0)}_{4,\rho} = -g_\rho h^{(0)}_\rho (1+\mu_v)$	4.850	14.94
$F^{(0)}_{5,\rho} = -g_\rho h^{(0)}_\rho$	1.032	3.180
$F^{(0)}_{6,\omega} = -g_\omega h^{(0)}_\omega (1+\mu_s)$	1.038	1.408
$F^{(0)}_{7,\omega} = -g_\omega h^{(0)}_\omega$	1.179	1.6
$F^{(1)}_{0,\rho} = -\frac{1}{2} g_\rho h^{(1)}_{\rho'}$	0.307	0.0
$F^{(2)}_{8,\rho} = -\frac{1}{2\sqrt{6}} g_\rho h^{(2)}_\rho$	0.886	2.542
$F^{(2)}_{9,\rho} = -\frac{1}{2\sqrt{6}} g_\rho h^{(2)}_\rho$	0.189	0.541

The expression of the coefficients $F^{(\Delta T)}_{k,s}$ multiplying the matrix elements $M^{(\Delta T)}_{k,s}$ (see eq.(14)) is reminded in the first column. Numerical values (in units of 10^{-6}) are given for the «best» values of the PNC meson-nucleon couplings in the DDH approach [13], as well as for the values obtained by Kaiser and Meissner [15].

strong coupling constants also). The second column contains the often used Desplanques, Donoghue, Holstein (DDH) [13] «best» values obtained within a quark plus Weinberg–Salam model. In the third column the fitted from experiments values of $h_m^{(\Delta T)}$ by Adelberger and Haxton [16] are listed. In the last column the values obtained by Dubovik and Zenkin (DZ) [14] within a more sophisticated quark plus Weinberg–Salam ($SU(2) \otimes U(1) \otimes SU(3)_C$) model are included. We consider these values as more «reasonable» values, taking into account that they are substained by comparison with the experimental data, given in the comprehensive review of Adelberger and Haxton (AH) [16].

The Kaiser and Meissner [15] approach is based on the soliton picture of the baryons, which takes into account important non-perturbative effects of QCD at low energies. The fact that the baryons may emerge as solitons from an effective meson Lagrangian with its intriguing connections to the chiral anomalies was suggested by Skyrme [83] and it has met with remarkable success in a variety of applications [89], [86], [85], [87], [88]. The Skyrme model deals with an effective theory of mesons, specifically with pions, and with the problem how to obtain baryons and their interactions in such a theory. The broad interest to this model found recently in the theory of strongly interacting particles is due to the speculations that effective theories of mesons may provide a link between QCD and the familiar picture of baryons interacting via meson exchange. This last picture has proven very useful in the past for energies up into the GeV region, because in this «low» energy domain QCD becomes forbiddingly difficult due to the rising coupling constants, which poses a major obstacle to a satisfactory description of the dynamical behaviour of the elementary quark and gluon fields of QCD at the relevant large distances. Some nonlinear field theories may have special solutions (solitons) and this leads to the Witten's suggestion [84] that baryons may be regarded as soliton solutions of the effective meson theory without any further reference to their quark content. This approach includes two distinct aspects: 1) the relation of the form of the effective non-linear meson theory to QCD and 2) the treatment of the structure of the baryons, which results from the effective Lagrangians, their interactions among themselves and their interactions with antibaryons or with mesons. Fortunately the second aspect may be considered quite independently from an eventual answer to the first question, which is quite difficult at the moment, because the underlying symmetries and the restrictions to low energies put limitations on the possible forms of the effective Lagrangians. Most of the results are assumed not to depend on the specifics of the chosen Lagrangian at all but will simply reflect symmetries and the fact that baryons are considered as soliton configurations in the basic meson field theory. Of course, not knowing the true effective theory we cannot expect quantitative agreement with the experimental data, however, if the whole concept is to make sense, we

should certainly expect that essential features of baryon structure and interactions should at least qualitatively be reproduced. In addition to the above-mentioned sources of incertitudes in calculating the weak meson-nucleon coupling constants ($h^{(\Delta T)}_{\text{meson}}$), the chiral-soliton treatment of the problem, in spite of its nonperturbative aspect, contains other shortcomings such like: a simplified quantization procedure, leading to higher masses and strong coupling constants for the nucleons, restrictions to two-flavor sector, the three-flavor sector being more appropriate because of possible strangeness admixtures to the proton wave functions.

Such a controversy greatly stimulates the investigation of possible experiments sensitive to the value of $h^{(1)}_{\pi}$.

The, usually known, PNC-NN potential [29] has the following form:

$$H_{PNC} = \sum_{\Delta T,\, s = \pi,\, \rho,\, \omega} V_s^{PNC}(\Delta T) = \sum_{\Delta T,\, k,\, s = \pi,\, \rho,\, \omega} F^{\Delta T}_{k,s} f^{\Delta T}_{k,s}, \tag{6}$$

where $V_s^{PNC}(\Delta T)$ are different meson contributions to the total PNC-NN potential (H_{PNC}):

$$V_{\pi}^{PNC}(\Delta T = 1) = \frac{1}{2\sqrt{2}} g_{\pi} h^{(1)}_{\pi} f^{(1)}_{0,\pi},$$

$$V_{\rho}^{PNC}(\Delta T = 1) = -\frac{1}{2} g_{\rho} h^{(1)}_{\rho} [f^{(1)}_{1,\rho} - f^{(1)}_{3,\rho} + (1 + \mu_v) f^{(1)}_{2,\rho}],$$

$$V_{\omega}^{PNC}(\Delta T = 1) = -\frac{1}{2} g_{\omega} h^{(1)}_{\omega} [f^{(1)}_{1,\omega} + f^{(1)}_{3,\omega} + (1 + \mu_s) f^{(1)}_{2,\omega}],$$

$$V_{\rho'}^{PNC}(\Delta T = 1) = -\frac{1}{2} g_{\rho} h^{(1)}_{\rho'} f^{(1)}_{0,\rho},$$

$$V_{\rho}^{PNC}(\Delta T = 0) = -g_{\rho} h^{(0)}_{\rho} ((1 + m_v) f^{(0)}_{4\rho} + f^{(0)}_{5\rho}),$$

$$V_{\omega}^{PNC}(\Delta T = 0) = -g_{\omega} h^{(0)}_{\omega} ((1 + m_s) f^{(0)}_{6\omega} + f^{(0)}_{7\omega}),$$

$$V_{\rho}^{PNC}(\Delta T = 2) = -\frac{1}{2\sqrt{6}} g_{\rho} h^{(2)}_{\rho} ((1 + \mu_v) f^{(2)}_{8\rho} + f^{(2)}_{9\rho}) \tag{7}$$

in which

$$f^{(1)}_{0,s} = \frac{1}{2M_N} i\, [\boldsymbol{\tau}_1 \times \boldsymbol{\tau}_2]_z\, (\boldsymbol{\sigma}_1 + \boldsymbol{\sigma}_2) \cdot \mathbf{u}(\mathbf{r}, m_s),$$

$$f^{(1)}_{1,s} = \frac{1}{2M_N} (\tau_{1_z} + \tau_{2_z})(\boldsymbol{\sigma}_1 - \boldsymbol{\sigma}_2) \cdot \mathbf{v}(\mathbf{r}, m_s),$$

$$f^{(1)}_{2,s} = \frac{1}{2M_N} (\tau_{1_z} + \tau_{2_z})\, i(\boldsymbol{\sigma}_1 \times \boldsymbol{\sigma}_2) \cdot \mathbf{u}(\mathbf{r}, m_s),$$

$$f^{(1)}_{3,s} = \frac{1}{2M_N}(\tau_{1_z} - \tau_{2_z})(\sigma_1 + \sigma_2) \cdot \mathbf{v}(\mathbf{r}, m_s),$$

$$f^{(0)}_{4,s} = \frac{1}{2M_N}(\tau_1 \cdot \tau_2)\, i\,[\sigma_1 \times \sigma_2] \cdot \mathbf{u}(\mathbf{r}, m_s),$$

$$f^{(0)}_{5,s} = \frac{1}{2M_N}(\tau_1 \cdot \tau_2)(\sigma_1 - \sigma_2) \cdot \mathbf{v}(\mathbf{r}, m_s),$$

$$f^{(0)}_{6,s} = \frac{1}{2M_N}\, i\,[\sigma_1 \times \sigma_2] \cdot \mathbf{u}(\mathbf{r}, m_s),$$

$$f^{(0)}_{7,s} = \frac{1}{2M_N}(\sigma_1 - \sigma_2) \cdot \mathbf{v}(\mathbf{r}, m_s),$$

$$f^{(2)}_{8,s} = \frac{1}{2M_N}[3\tau(1)_z\, \tau(2)_z - \tau(1) \cdot \tau(2)]\, i[\sigma(1) \times \sigma(2)] \cdot \mathbf{u}(\mathbf{r}, m_s),$$

$$f^{(2)}_{9,s} = \frac{1}{2M_N}[3\tau(1)_z\, \tau(2)_z - \tau(1) \cdot \tau(2)][\sigma(1) - \sigma(2)] \cdot \mathbf{v}(\mathbf{r}, m_s) \tag{8}$$

with

$$\mathbf{u}(\mathbf{r}, m_s) = \left[(\mathbf{p}_1 - \mathbf{p}_2), \frac{1}{4\pi r} \exp(-m_s r) \right]_- \tag{9}$$

$$\mathbf{v}(\mathbf{r}, m_s) = \left\{ (\mathbf{p}_1 - \mathbf{p}_2), \frac{1}{4\pi r} \exp(-m_s r) \right\}_+ . \tag{10}$$

Here

$$g_\pi = 13.45,\ g_\rho = 2.79,\ g_\omega = 8.37,\ \mathbf{r} = \mathbf{r}_1 - \mathbf{r}_2,\ \mu_v = 3.7 \text{ and } \mu_s = -0.12.$$

Recently, it was proposed [96] a new parity violating mechanism, specific for nucleons bound in the nucleus and it was shown that this mechanism generates a new term in H_{PNC} sometimes of the same order as the above proposed terms. This mechanism consists of weak emissions and absorptions of mesons by a single nucleon in the presence of the strong nuclear field. This PNC process is forbidden for a free nucleon by the time reversal invariance, it can occur, however, for a nucleon interacting with a nuclear field. A similar situation occurs in quantum electrodynamics, where the interaction of a bound electron with the radiation field leads to a modification of the Coulomb potential, responsible for the well-known Lamb shift [97].

The shape of this single particle PNC interaction potential depends on the choice of the relativistic potential $V^\mu \cdot S$ (see Ref. [98]):

$$S = \left(\frac{1}{2} U_0 - 2M^2 r_0^2 U_{ls} \right) \cdot f(r);$$

$$V^0 = \left(\frac{1}{2} U_0 + 2M^2 r_0^2 U_{ls} \right) \cdot f(r); \qquad V^i = 0; \quad i = 1, 2, 3 \tag{11}$$

decsribing the external field and not on the nature of the exchanged meson. Its expression is [96]:

$$V_{PNC}^{CM} = \frac{(\alpha T)^s}{M^2} \left(\frac{U_0}{4M} + U_{ls} M r_0^2 \right) \{ \boldsymbol{\sigma} \cdot \mathbf{p}, \Delta f(r) \}. \tag{12}$$

Here $\mathbf{p}$ denotes the momentum operator of the nucleon. The (αT) coupling constants depend on $h_{\text{meson}}^{(\Delta T)}$: $h_\pi^{(1)}$, $h_\rho^{(0)}$, $h_\rho^{(1)}$, $h_\rho^{(2)}$, $h_{\rho'}^{(1)}$, $h_\omega^{(0)}$, $h_\omega^{(1)}$ and sometimes on τ_3-component of the isospin. This new PNC term (12) should be added to the PNC matrix elements with no isospin change and, hence, it does not contribute to the isovector PNC matrix elements. A crude estimation of the magnitude of this new contribution to H_{PNC}, e.g. of the term containing the $h_\rho^{(1)}$ is given in the following. Defining the ratio between the $M_{PNC}^{CM}(h_\rho^{(0)})$ and $M_{PNC}^{DDH}(h_\rho^{(0)})$ by R, Caprini and Micu [96] found $R = \dfrac{24}{9\gamma A^{2/3}}$, where γ is an overall reduction factor due to short range correlations, ratio, which, for instance in the case of ^{14}N PMD1 is $\simeq 1/4$.

In view of these results it may be interesting to reconsider other meson exchanges than those permitted by Barton's theorem [82].

3. SHELL MODEL PREDICTIONS FOR PARITY MIXING MATRIX ELEMENT

The calculation of the PNC effects in the nucleus is usually divided into four parts. The first part belongs to the elementary particle physics. In this part the weak $(h_{m-N}^{(\Delta T)})$ and strong (g_{m-N}) meson-nucleon coupling constants are calculated starting from the quark structure of the hadrons and their elementary interactions [13], [14] or by applying effective theories of mesons and baryons [85], [86], [88], [89], [87], such as the soliton picture of the nucleon [15], which takes into account important non-perturbative effects of QCD at low energies. These coupling constants enter as input in the second part of the analysis, where the quantum fluctuations consisting of meson emissions and absorptions in the nucleus are explored and their effects are expressed as an equivalent non-relativistic PNC nuclear Hamiltonian (H_{PNC}). The shape of the

PNC interaction potential (H_{PNC}) is determined by the nature of the exchanged meson, while the information related to the weak interaction vertex, the most unknown part, is contained in seven coupling constants $h^{(\Delta T)}_{\text{meson}}$: $h^{(1)}_{\pi}$, $h^{(0)}_{\rho}$, $h^{(1)}_{\rho}$, $h^{(2)}_{\rho}$, $h^{(1)}_{\rho'}$, $h^{(0)}_{\omega}$, $h^{(1)}_{\omega}$. In the third part we need nuclear matter techniques. To compute the PNC matrix elements (M_{PNC}) of H_{PNC} between nuclear wave functions we need to evaluate the short range correlations (SRC) [90], [91], [100], [99], which describe the effect of the distortion of the relative two-nucleon wave functions at small distances due to the strong repulsive core in the nuclear interactions. The repulsion punches a hole in the relative two-nucleon wave functions, near the origin and this has strong effects on two-body observables, as, e.g., those generated by H_{PNC}, which is of very short range (less 1.5 fm, while the core radius is $\simeq 0.5$ fm). The SRC act as a renormalization of H_{PNC} [20]. The matrix elements of this «renormalized» potential between nuclear wave functions are finally evaluated (the fourth part), in order to obtain predictions for measurable quantities, such as rates of forbidden transitions (pseudoscalar observables: *PNC asymmetries, analyzing powers and circular polarizations* or directly the PNC-decay rates as, e.g., the PNC-α-decay rates, [16], [17], [44], [22], optical rotation parameters [21], etc.). Particularly the OXBASH shell model code in the Michigan State University version [63], [117], [111], [112], [25], [24], [57], [113], [114], [115], [116], [118] is situated along the fourth step of the above-mentioned program.

In order to determine the range and the amplitude of the PNC observables around the excitation energy of the PMD's we have made a shell model estimate of the PNC matrix element using the OXBASH code, which includes different model spaces and different residual effective two-nucleon interactions

$$M_{PNC} = \langle J^{-\pi} T, E_x(\text{MeV}) \,|\, H_{PNC} \,|\, J^{\pi} T', E'_x(\text{MeV}) \rangle =$$

$$= \sum_{\Delta T, k, s = \pi, \rho, \omega} F^{(\Delta T)}_{k,s} M^{PNC}_{\Delta T, k, s}, \tag{13}$$

where

$$M^{PNC}_{\Delta T, k, s} = \langle J^{-\pi} T, E_x(\text{MeV}) \,|\, f^{(\Delta T)}_{k,s} \,|\, J^{\pi} T', E'_x(\text{MeV}) \rangle \tag{14}$$

are different (see eq. 8) nuclear stucture matrix elements (in MeV).

To obtain the effective two-body interactions (ETBI) we can, e.g., use the *G*-matric method [73], [74], [102], [103], [75], [99], [100], [101] by solving the generalized Bethe–Goldstone [99] or Bethe–Faddeev [100] equations. The method is iterative [101]:

1) first, a complete set of single-particle (s.p.) states is chosen (in the OXBASH-code, s.p. oscillator states are chosen);

2) the reaction G-matrix is then calculated and a first iterated ETBI is obtained;

3) the Hartree–Fock (HF) equation with this ETBI is solved to yield a first iteration of the occupied s.p. energies and wave functions;

4) the generalized Bethe–Goldstone and Bethe–Faddeev eqs. are solved in order to establish the unoccupied state potential;

5) the Schroedinger eq. for the unoccupied s.p. energies and wave functions is solved;

6) the unoccupied s.p. basis is orthogonalized to the occupied s.p. states found at step 3) to give the first iteration to the unoccupied s.p. states.

Having in such a way a complete set of first iterated s.p. states we repeat a second cycle starting with the step 2). After a number of iterations, depending on the fact how good were the first chosen s.p. basis and G-matrix, we obtain the last iterated s.p. basis and the ETBI.

The ETBI obtained in such a way is diagonalized in the last iterated s.p. basis (m-scheme) or in a more sophisticated basis obtained by different coupling and projection procedures [113].

The ETBI and the s.p. basis parameters can be extracted from experimental data also.

Our calculations use both procedures.

In these calculations the ZBM, PSD, D3F7 and SDPFW model spaces have been used.

Let us denote the shell model orbits as follows:

orbits	$1s_{1/2}$	$1p_{3/2}$	$1p_{1/2}$	$1d_{5/2}$	$1d_{3/2}$	$2s_{1/2}$	$1f_{7/2}$	$2p_{3/2}$	$2p_{1/2}$
number	1	2	3	4	5	6	7	8	9

In these calculations the ZBM, PSD, D3F7 and SDPF model spaces have been used:

model space	filled orbits	valence orbits
ZBM	1,2	3,4,6
PSD	1	2,3,4,5,6
D3F7	1,2,3,4	5,7
SDPF	1,2,3	4,5,6,7,8,9

The abbreviation ZBM should be understood as the Zucker–Buck–McGrory model space [76]. In Ref. [76] the single particle energies were fitted to the values obtained from the experiment, and the two-body-matrix-elements (TBME) were identified with Kuo and Brown *G*-matrix elements (the *F*-interaction abbreviated as ZBMI) [71], [72], [25]. Within the ZBMII we are dealing

with the same model space as above. A fitting procedure for two single particle energies and for 30 TBME in the $A = 13 \div 17$ mass region was performed (the *Z*-interaction) [25], [76], [77]. REWIL makes a 33 parameter fit of spectra in $A = 13 \div 22$ mass region [104]. In the ZWM and ZBMO the two-body matrix elements are calculated by using a Hamada–Jonston *G*-matrix [112] and the Oxford Avila–Aguirre–Brown [63] interactions, respectively. The centre of mass spurious component in the wave functions has been eliminated according to the prescription given in Ref. [118].

Within PSDMK the PSD model space is used and the interactions as follows: — for P-space the Cohen–Kurath interaction [105] — for SD-space the Preedom–Wildenthal interaction [106] — for the coupling matrix elements between P- and SD-spaces the Millener–Kurath interaction [107] very close to the G-matrix one is used. PSDMWK uses the same PSD model space and the only change as compared to PSDMK is that in the SD-space the Wildenthal [114] interaction is used.

Within the D3F7 model space the single particle energies and the two-body matrix elements were fitted. In the calculations we denoted different interactions as follows. The HW-interactions stands for the Hsieh–Wildenthal interaction [63], WO and W4 — for another Wildenthal inetarction as used in [115] and [1114], respectively and FEPQ stands for the Federman–Pittel interaction [116].

In the calculations within the SDPF of the natural parity states the restriction to the sd major shell was enough to be considered.

In most of the cases there are two types of contributions to the PNC matrix element: one is coming from two-body transition densities (TBTD) if all four orbitals entering the two-body matrix elements (TBME) are in the valence space [25]; another one arises from the one-body transition densities (OBTD) if two orbitals are in the core. For instance, in the case of ^{16}O PMD1 the only contribution to the latter one comes from the following matrix element:

$$\langle (1s_{1/2})^4 (1p_{3/2})^8 \, 2s_{1/2} \| H_{PNC} \| (1s_{1/2})^4 (1p_{3/2})^8 \, 1p_{1/2} \rangle \qquad (15)$$

which turns out to be the dominant one in all described cases.

3.1. Short Range Correlations. Since all the components [13], [16] of H_{PNC} are short range two-body operators and bearing in mind that the behaviour of the shell model wave functions at short relative *NN* distances is wrong, it is necessary to use shell model wave functions including short range correlations (SRC) to calculate correctly their matrix elements. The correlations were included by multiplying the harmonic oscillator wave functions (with $\hbar\omega = \frac{41}{A^{1/3}}$ MeV) by the Jastrow factor:

$$1 - \exp(-ar^2)(1 - br^2); \quad a = 1.1 \text{ fm}^{-2}; \quad b = 0.68 \text{ fm}^{-2} \tag{16}$$

given by Miller and Spencer [65]. This choice is consistent with results obtained by using more elaborate treatments of SRC such as the generalized Bethe–Goldstone approach [66], [67], [20] and should roughly correspond to a *NN*-interaction close to the Reid-soft-core model for the $^1S_0$ and $^3P_0$ components. The comparison with more recent models of the *NN* strong interactions [68] indicates that the Miller and Spencer approach (16) overestimates the effect of short range repulsion. From inspection of the $^3S_1$-component of the deuteron wave function, one thus expects that the correlation function does not vanish at the origin. With the same asymptotic normalization as in (16), it would be close to 0.1 for the Paris model [69] and 0.5 of the Bonn model [68]. Moreover, the correlation function (16) neglects the effect of the tensor force, which admixes to the $^3S_1$-state a $^3D_1$-component, that has also a short range character. This effect is large and, depending on the transition amplitude, it is constructive or destructive [137]. In the case of the π-exchange contribution, dominated by the $^3P_1$-$^3S_1(+\,^3D_1)$ transition, it compensates a large part of the short range repulsion [137]. In the contrary, in the case of the isoscalar ρ-exchange contribution, *a priori* dominated by the $^1P_1$-$^3S_1(+\,^3D_1)$ transition, it provides further suppression.

The above improvements should be incorporated in definitive predictions. We will not do it and will stick to (16). First, there is no end to playing with different models of short-range correlations. Second, there are other possible improvements due, for instance, to the part of the exchange of a 2π contribution not included in the ρ, to vertex form factors, to heavier meson exchanges, etc. Furthermore, the corresponding uncertainties will add to those on the PNC coupling constants themselves. In our mind, it is more important to make predictions that can be compared to other ones than to multiply them by looking at modifications of rather-minor relevance at the present time. The essential point is that the PNC potential given by (6) can account independently for the various contributions expected to dominate at low energy which are due to the PNC-NN transition amplitudes $^1S_0$-$^1P_0$ (3 amplitudes: *pp*, *nn* and *pn* or $\Delta T = 0$, 1 and 2), $^3S_1$-$^3P_1$ (*pn*, $\Delta T = 0$) and $^3S_1$-$^3P_1$ (*pn*, $\Delta T = 1$). A few clues as to the relevance of these amplitudes will be given when discussing the results.

By including SRC the PNC pion exchange matrix element decreases by $40 \div 50$ without including SRC, while the ρ(ω) exchange matrix elements also decrease by a factor of $1/3 \div 1/7$.

3.2. The Lanczos Technique. The OXBASH-code includes a powerful algorithms based on the work of Lanczos [108], [109]. Some of the techniques we use might be equally effective for some heavy nuclear regions and high spin, particularly when the spin is close to the limiting value in the chosen shell model space.

The basic tool, the Lanczos algorithm, allows one to find the extremum (lowest and highest) eigenvalues and associated eigenvectors of a very large matrix iteratively. With standard workstations, matrices of dimension $\simeq 10^6$ by 10^6 can be treated in this way. In constrast, standard methods for fully diagonalizing matrices are usually limited to about 10^3 by 10^3 [110]. An even more powerfull aspect of this algorithm, due to its connections with the method of moments, is that it can be used to generate inclusive response functions and Green's functions iteratively. Thus the Lanczos algorithm has proven useful in a wide variety of the problems, including nuclear shell model, atomic and molecular structure, spin-lattice problems in condensed matter physics, and Hamiltonian lattice gauge theory. In what follows we sketch the algorithm, especially for nuclear structure applications.

Consider a Hamiltonian H, defined over a finite Hilbert of dimension N, and a starting normalized vector $|\psi_1\rangle$ in that space. We begin to construct a basis for representing

$$H = \sum_{mn} |\psi_n\rangle H_{mn} \langle \psi_m| \tag{17}$$

by

$$H|\psi_1\rangle = \alpha_1 |\psi_1\rangle + \beta_1 |\psi_2\rangle, \tag{18}$$

where $|\psi_2\rangle$ is a normalized vector representing that part of $H|\psi_1\rangle$ orthognal to $|\psi_1\rangle$, i.e.,

$$\beta_1 |\psi_2\rangle = \sum_{n \neq 1} H_{1n} |\psi_n\rangle; \quad \alpha_1 = H_{11}. \tag{19}$$

Proceeding

$$H|\psi_2\rangle = \beta_1 |\psi_1\rangle + \alpha_2 |\psi_2\rangle + \beta_2 |\psi_3\rangle, \tag{20}$$

$$H|\psi_3\rangle = \beta_2 |\psi_2\rangle + \alpha_3 \psi_3\rangle + \beta_3 |\psi_4\rangle \tag{21}$$

and so on. Note that the term $\beta_1 |\psi_1\rangle$ must appear in the first line above because H is Hermitian. Also note that $|\psi_1\rangle$ does not appear in the second line above because everything that connects to $H|\psi_1\rangle$ other than $|\psi_1\rangle$ is defined as $|\psi_2\rangle$. Similarly, $H|\psi_4\rangle$ will contain nothing proportional to $|\psi_1\rangle$ or $|\psi_2\rangle$. Thus H has been cast in a tridiagonal form:

$$H = \begin{pmatrix} \alpha_1 & \beta_1 & 0 & 0 & .. \\ \beta_1 & \alpha_2 & \beta_2 & 0 & .. \\ 0 & \beta_2 & \alpha_3 & \beta_3 & .. \\ 0 & 0 & \beta_3 & \alpha_4 & .. \\ .. & .. & .. & .. & .. \end{pmatrix}. \tag{22}$$

As an example, within ZBM [76] — model space as $|\psi_1\rangle$-starting vector, one can use one from the following vectors:

$$\left| \left\{ [(1d_{5/2})^{n_1}_{I_1 T_1} \cdot (2s_{1/2})^{n_2}_{I_2 T_2}]^{(n_1+n_2)}_{I_{12} T_{12}} \cdot (1p_{1/2})^{n_3}_{I_3 T_3} \right\}^{(\sum_{i=1}^{3} n_i)=4}_{IT} \right\rangle \tag{23}$$

constructed within an oscillator single particle basis.

If this procedure is continued for N steps, the full H would then be in tridiagonal form. However, the power of the algorithm derives from the information in the tridiagonal Lanczos matrix when the procedure is truncated after n iterations, $n << N$. If Ψ_{E_i}, $(i = 1, ..., N)$ are the exact eigenfunctions of H, then

$$\langle \psi_1 | H^{\lambda} | \psi_1 \rangle = \sum_{i=1}^{N} |\langle \psi_1 | \Psi_{E_i} \rangle|^2 E_i^{\lambda} \equiv \sum_{i=1}^{N} f(E_i) E_i^{\lambda}. \tag{24}$$

The distribution $f(E_i)$, $(i = 1, ..., N)$ can be thought of as a set of N weights f and measures E_i (the eigenvalues) characterizing the distribution of $|\psi_1\rangle$ in energy, i.e., the f's determine a complet set of moments. The truncated Lánczos matrix, when diagonalized, provides the information needed to construct a distribution $g(\tilde{E}_i)$, $(i = 1, ..., n)$ with $\tilde{E}_i \simeq E_i$, which has the same $2n + 1$ lowest moments in E as the exact distribution $f(E_i)$, $(i = 1, ..., N)$. In other words, the Lanczos algorithm provides, at each iteration, a solution to the classical moments problem [109].

4. ASYMMETRIES IN RESONANCE ELASTIC SCATTERING AND NUCLEAR REACTIONS

As a rule, in studying nuclear collisions induced by polarized projectiles that populate a PMD occuring in the compound nucleus excitation spectrum [64], the largest magnitude of the PNC effects can be observed [56], [31], [32], [33] for the projectile energy around the member of the PMD having the smallest (Γ_c^{small}) partial width (*a narrow resonance*).

In the vicinity of this narrow resonance the PNC analyzing powers (A_L and A_b [34], [35], [41], [42], [37], [55], [54], alternatively the index $L(b)$ can be found as $z(x)$ in other works) have the following simple expression:

$$A_{L(b)} = D_{L(b)} \frac{1}{2} \Gamma^{\text{small}} \left(E - E^{\text{small}} + \frac{i}{2} \Gamma^{\text{small}} \right)^{-1} \exp\left(i(\varphi_{L(b)} + \varphi_{PNC})\right), \quad (25)$$

where

$$D_{L(b)} = 2 \frac{|M_{PNC}|}{|(E - E^{\text{large}} + i/2\Gamma^{\text{large}})|} \sqrt{\frac{\Gamma_c^{\text{large}}}{\Gamma_c^{\text{small}}}} |C_{L(b)}| \quad (26)$$

and

$$C_{L(b)} = |C_{L(b)}| \, e^{(i\varphi_{PC}^{L(b)})} = \frac{|(E - E^{\text{large}} + i/2\Gamma^{\text{large}})|}{\sqrt{\Gamma^{\text{large}} \Gamma^{\text{small}}}} \cdot \quad (27)$$

$$\frac{\Sigma_l P_l^{(\kappa)}(\cos\theta)[\Sigma_n c'_n(L(b)) \, iC(\theta) \, \tilde{t}_n^* + \Sigma_{mn} b_{mn}^l(L(b))(\tilde{t}_m t_n^* + \tilde{t}_m^* t_n)]}{\Sigma_l P_l(\cos\theta) \Sigma_{mn} a_{mn}^l t_m t_n^*}$$

is a function on the PC transition matrix elements only (for L: $\kappa = 0$, for b: $\kappa = 1$, and, e.g., for the proton channel (p) we use the notations $\tilde{t}_n = T^{PC}_{pls,\, pl_1 s_1}$) $\exp(i(\xi_{pls} - \xi_{pl's'}))$. The coefficients $a_{mn}^{(l)}(L(b))$, $b_{mn}^{(l)}(L(b))$ and $c_n^{(l)}(L(b))$ are simple specific values of the geometrical coefficients for the case we are investigating [34], [35], [41], [42], [37], [55], [54].

The largest energy anomaly ($\Delta A_{L(b)}$), i.e., the distance between the minimum and the maximum of the PNC analyzing powers of the excitation function in the vicinity of the narrow resonance level is equal to the quantity $D_{L(b)}$ above defined and it does not depend on the PNC matrix element phase — φ_{PNC} and PC quantity phase — $\varphi_{L(b)}$ [34]:

$$D_{L(b)} = D^0_{L(b)} \Big| \sum_{\Delta T,\, s = \pi,\, \rho,\, \omega} V_s^{PNC}(\Delta T) \Big| = D^0_{L(b)} \Big| \sum_{\Delta T,\, k,\, s} F_{k,\, s}^{(\Delta T)} M_{k,\, s}^{(\Delta T)} \Big|, \quad (28)$$

where $V_s^{PNC}(\Delta T)$ (in eV) are different meson contributions to the total PNC shell model matrix element. The $F_{k,\, s}$ in units of 10^{-6} are given in Table 3 (see also Table 2 of Ref. [23]). The $M_{k,\, s}$ are nuclear structure matrix elements in units of MeV.

The quantity $D_{L(b)}$ (in eV^{-1})

$$D_{L(b)}^{(0)} = 2\left(E - E^{\text{large}} + \frac{i}{2}\Gamma^{\text{large}}\right)^{-1} \sqrt{\frac{\Gamma_p^{\text{large}}}{\Gamma_p^{\text{small}}}}\,|C_{L(b)}|. \tag{29}$$

4.1. Parity Mixing in ^{14}N. In the excitation spectrum [64] of the ^{14}N nucleus there are two PMD's lying at 8.7 MeV and 9.3 MeV excitation energy (see Table 1).

The difference between the two PMD's is that the PMD1 is essentially of the isoscalar type, while the PMD2 is of the isovector type, hence, an interesting case for searching the neutral currents in the structure of the weak hadron-hadron interaction.

There is only one experiment concerning the PNC effects in ^{14}N-nucleus. In the following we try to explain this Seattle–Madison [56] experiment about the PNC effect around the first PMD in ^{14}N investigated via ^{13}C(**p**, p)^{13}C resonance scattering. The only possible measured quantity was the longitudinal analyzing power. The experimental apparatus was developed with symmetry and stability as major design considerations. The maximum count rate attainable for this experiment was governed by the 3.8 keV width of the 0^+1 resonance, since the optimum target thickness is of that order and the maximum current on target was less than $1\mu A$. The experiment could be done by counting the scattered protons individually (expected rates less than $1MHz$). Since the elastic scattering is the only open particle decay channel, the detector resolution was sacrificed for speed. It was used thin plastic scintilators mounted on 5.1 cm PMT's. The relevant features of the detectors:~10 nsec pulsewidth, ~25—30% resolution, a stiff base current to gain stability, robustness toward radiation damage, and large solid angle. It was used a four-fold (left-right, up-down) detection geometry with eigth detectors azimuthally symmetric about the beam axis, four at $\theta_1 = 35°$ and four at $\theta_2 = 155°$. The maximum PNC signal was expected to be the difference: $A_L(\theta_2) - A_L(\theta_1) = A_L(b-f)$ (the back-front PNC signal). In such a detection scheme there should be small systematic asymmetries due to position and angle modulations that may be correlated with the beam helicity reversal. The back-front PNC signal gives the self-normalizing system and desensitizes the detector to small target thickness variations. A target rastering device is used in order to desensitize the detectors to the target irregularities. The long-term correction capabilities, for a typical two week run, lead to the fact that the transverse asymmetries are kept to a level of $\overline{P}_T A_T < 2 \cdot 10^{-5}$. Because of the energy modulations due to the beam helicity reversal the measured sensitivity was $\delta A_L(b-f)/\delta E = 9 \cdot 10^{-5}$/ eV; statistical accuracy of $\Delta E = 0.2$ eV was

achieved with 1.5 days of running time. Several measurements were taken giving no clear indication of any energy modulation. The measured beam parameters, sensitivities of the apparatus and the false asymmetries are:

Systematic contributions to A_L from coherent beam modulations

Quantity	Measured Value	Sensitivity*	Resulting False Asymmetry
		Spin Independent Effects	
Intensity $(\Delta I/2I)$	$\leq 5\cdot10^{-4}$	$-2.1\cdot10^{-3}$	$\leq 1.0\cdot10^{-6}$
Position	$(5\pm2)\cdot10^{-4}$ mm	$-1\cdot10^{-4}/\text{mm}^2$	$\leq 1.2\cdot10^{-8}$
Angle	—	$-1.7\cdot10^{-7}/\text{mrad}^2\cdot\alpha$	—
Width $(\Delta\Gamma/\Gamma)$	$< 2\cdot10^{-3}$	$7.5\cdot10^{-4}$	$< 1.5\cdot10^{-6}$
Energy	0.3 ± 0.6 eV	$2\cdot10^{-6}$/eV	$(0.6\pm1.2)\cdot10^{-6}$
		Spin Dependent Effects	
$(\langle\boldsymbol{\varepsilon}\rangle\cdot\langle\mathbf{p}\rangle)\cdot\hat{z}$	$< 2.5\cdot10^{-4}$ mm	$-5.5\cdot10^{-4}/\text{mm}$	$< 1.4\cdot10^{-7}$
$\langle\boldsymbol{\alpha}\rangle\cdot\langle\mathbf{p}\rangle$	$< 6\cdot10^{-4}$ mrad	$2.4\cdot10^{-4}/\text{mrad}$	$< 1.4\cdot10^{-7}$
$\langle\varepsilon_x p_y\rangle - \langle\varepsilon_y p_x\rangle$	≈ 0.02 mm	$-6.7\cdot10^{-5}/\text{mm}$	$\approx 1.3\cdot10^{-6}$
$\langle\alpha_x p_x\rangle - \langle\alpha_y p_y\rangle$	—	$2.0\cdot10^{-5}/\text{mrad}$	—

$\hat{z}$ — nominal chamber axis, $\boldsymbol{\varepsilon}$ — displacement of beam on target from z-axis, $\boldsymbol{\alpha}$ — angle of beam on target from z-axis, $\mathbf{p}$ — polarization vector.

*Sensitivities are for E_p (lab) = 1158 keV, 25μ gm/cm^2 ^{13}C target.

Fortunately there exists a «magic» energy where the sensitivity of both the transverse polarization gradients and of energy modulation roughly vanishes. The resulting longitudinal analyzing power is: $A_L(b-f) = (0.86\pm0.59)\cdot10^{-5}$ with a systematic error estimate of $0.24\cdot10^{-5}$.

The original calculations ($A_L \approx -2.8\cdot10^{-5}$) [55] on which the PMD1 experiment in ^{14}N system was based lead to an isoscalar constraint of opposite sign to the DDH prediction [56] and are in better agreement to the ^{21}Ne than in ^{19}F cases, if consider the nuclear part of the calculations without problems. It is interesting that in this case the theoretical value of the PNC matrix element decreased along the time from 1.37 eV (obtained within a restricted REWIL space [55], passing through the Haxton value 1.04 eV [56], [55] (addendum),

[127] (within full $\hbar\omega$) and to our value 0.5 eV (within the PSD model space) or smaller [39]. Before extracting a reliable value of $h_\rho^{(0)}$ coupling constant, we must have a confidence in the nuclear structure and reactions considerations (shell model, scattering theory) used to predict the PNC effect.

The predictions of the analyzing powers depend on the models for nuclear structure and nuclear reaction mechanisms. At present it is not known a unique model for both nuclear structure and nuclear reaction parts at the necessary level to describe PNC effects. Therefore, when we calculate the PNC observables by using formulae, such like those given in the Refs. [55], [54], [37], [41], [42], which should not depend on the phases of the wave function used, they in reality will depend on these phases, because we are forced to apply different models for different quantities entering the above formulae. As an example within the OXBASH code we calculate the PNC matrix elements and the spectroscopic amplitudes, but not the scattering phases and the partial widths, for which we are forced to apply models given by a specific nuclear reaction mechanisms. For the scattering phases we, for instance, should incorporate in the optical potential terms which are not directly present in the OXBASH-code, or at least they could have not the same form (as, e.g., the spin-orbit term or may be tensorial terms). The average field and the effective residual interactions, present in the OXBASH-code, are so prepared in order to work within a bound state basis. It does not contain continuum or resonance s.p. states or more complicated states, such as the continuum states for two or three reaction fragments. Moreover, the OXBASH-code is based on s.p. oscillator potential, which always produced bound states. Some other codes [119] are sometimes based on more realistic Saxon–Woods bound states basis, however, the continuum states are not incorporated in such codes also. The only approach, which takes care of both bound and continuum s.p. states, is the shell model approach to nuclear reactions [120], however, within this approach the residual interactions cannot be included easily and the PNC observables cannot be estimated without incorporating the residual interactions in the model calculations.

If using our PNC matrix element (0.5 eV), the agreement between the experimental and the theoretical magnitude of the largest energy anomaly ($\Delta A_{L(b)}$) is better, however neither in [55] nor in our work the contribution from the recently proposed in Ref.[96] s.p. PNC matrix element was calculated.

From these calculations we may learn: i) the PNC matrix element is dominated by the $h_\rho^{(0)}$-term. This becomes three times smaller in the Kaiser and Meisner chiral-soliton theory as compared to the DDH «*best values*» (see Table 2 for a comparison with other theories for weak vertices); ii) the refinements in the structure part of the PNC matrix element have been carefully discussed in Refs. [56] and [39]. The new s.p. term proposed by Caprini and Micu may

diminish the total PNC matrix element also. All these ingredients may reduce the total matrix element by 40% and the $h_\rho^{(0)}$ obtained in Ref.[16] could, in principle, describe the experimental data [56]; iii) a new measurement of the longitudinal analyzing power for this case is necessary to be performed in order to stengthen the conclusions based on the experimental value of Ref.[56]. The new measurement is proposed [121] to be done at an angle $\theta_{CM} = 100°$, where the quantity $\sigma(\theta_{CM}) \cdot A_L^2(\theta_{CM})$ (proportional to the measuring time for a defined precision) has a maximum in the backward region.

The PMD2 case has other problems. Because of the small width (0.135 KeV) of the 2^+1, 9.17225 MeV — level the energy anomaly of the PNC analyzing powers is a non-zero quantity in a very small [41] energy range (≤ 1 KeV) only, and it is of the order of some units above 10^{-5} within the DDH + PSDMK (Millener–Kurath interaction) [13] [63]. If considering the $2^\pm$ PMD in ^{14}N to be analysed via circular polarization of 9.3893 MeV γ-ray we came to realize that this observable is equal to $1.04 \cdot 10^{-3}$ in the case of an unoriented $2^-T = 0$ state and with zero mixing ratios. This value has been obtained by calculating, within OXBASH-code (Millener–Kurath-interaction), the 9.3893 MeV $E1 + M2$ γ-emission probability ($2.886 \cdot 10^{12} s^{-1}$) and the 9.17225 $M1 + E2$ γ-emission probability ($3.036 \cdot 10^{16} s^{-1}$). The last value ($\Gamma_\gamma = 24.4$ eV) is in agreement with the measured value ($\Gamma_\gamma = 7$ eV) [122]. Unfortunately there is not a measured value for the $E1 + M2$ γ-emission. This high value of the circular polarization, can be explained by a high hindered E1 transition, which is isospin forbidden. This measurement has, however, a very small probability, because of an almost 100% proton decay probability of the 2^-0, 9.3893 MeV state, however, it could be performed analogously to the ^{19}F experiment.

4.2. Parity Mixing in ^{16}O. The ^{16}O energy spectrum contains two (see Table 1) isovector PMD's [64] one PMD ($\Delta E \approx 50$ KeV) lying at 13 MeV excitation energy [34], [35] (see Table 4) and the second one ($\Delta E \approx 9$ KeV) is lying at 16.2 MeV excitation energy [42] (see Table 5).

These PMD's can be explored by measuring two components of the vector analyzing power — A_L and A_b for which, a careful theoretical analysis is done and the estimations are: $A_L^{PMD\,1} = 1.4 \cdot 10^{-5}$, $A_b^{PMD\,1} = 0.9 \cdot 10^{-5}$ [34], $A_L^{PMD\,2} = 3.2 \cdot 10^{-5}$ and $A_b^{PMD\,2} = 2.3 \cdot 10^{-5}$ [42] for large angles ($\simeq 150°$).

We want to discuss the first PMD in more detail, since it has been the subject of our group special attention [34] as the best candidate for a new

isovector experiment. The α_0-transition from the $J^\pi T = 2^- 1$ state in ^{16}O ($E_x = 12.9686$ MeV, $\Gamma_{cm} = (1.6 \pm 0{,}1)$ keV), populated by resonant capture of polarized protons ($E_p = 0.898$ MeV), to ^{12}C (g.s.) was thoroughly investigated theoretically [34]. This transition has originally been mentioned by Bizzeti and Maurenzig [123]. The α_0-transition is forbidden by parity and, partially, by isospin selection rules. It, therefore, can predominantly be described by the isovector part of the PNC-NN potential (mainly one pion exchange), thus being sensitive to the weak πNN coupling constant $h_\pi^{(1)}$.

The excitation functions of the PNC longitudinal (A_L) and PNC transverse (A_b) analyzing powers are expected [123], [54], [37], [55], [31], [32] to show an energy anomaly at the 2^-1 resonance energy due to the interference of the forbidden (PNC: 2^-1, 12.9686 MeV) and allowed (2^+0, 13.020 MeV; 1^-1, 13.090 MeV) resonance transition amplitudes as well as a (PC: 0^+0) background transition amplitude. The level structure of the ^{16}O nucleus [64] enhances the interference effect because of the close lying ($\Delta E = 51$ keV) broad overlapping 2^+0 state at $E_x = 13.020$ MeV with $\Gamma_{cm} = (150 \pm 10)$ keV.

Following Ref.[44], where a more rigorous approach to the parity forbidden alpha decay is proposed, it is possible to estimate the order of magnitude of the weight of the admixtures from different 2^+0 levels into the 2^-1 level as a product

$$F_n S_{\alpha n}^{1/2} = \left| (E^{2^-1} - E^{2^+0})^{-1} \langle 2^-1 | H_{PNC} | 2_n^+0 \rangle S_{\alpha n}^{1/2} \right| \qquad (30)$$

where $S_{\alpha n}^{1/2}$ is a SU(3) alpha particle amplitude [63]. The results are listed in Ref. [34]. From these values we conclude that the assumption of a parity mixed doublet (2^-1, 12.9686 MeV and 2^+0, 13.020 MeV excited states in ^{16}O) is justified. In this case, the expression for the PNC-T-matrices, obtained by expanding the exact Green's function [37], [55], [54] to first order in H_{PNC}, is certainly a good approximation. It is assumed that the projectile and the target are parity eigenstates. Then PNC contributions from direct reaction terms are ignored and only effects related to the closeness of the two resonances are taken into account. The resonance parameters for the quantities entering in eqs. for $A_{L(b)}$ are given in Ref.[34].

The parity mixing of the above mentioned doublet is of particular interest because:

(1) The mixing is sensitive to the $\Delta T = 1$ components of H_{PNC} and especially to the long range part described by weak pion exchange, taking the quark

model picture. In this case quantitative informations about neutral current contributions to H_{PNC} are expected. Several cases have been proposed theoretically, but only few of them have been experimentally investigated; only the ^{18}F experiment (average of 5 investigations) [16] gives a reliable upper limit for the weak pion-nucleon coupling constant. Taking into account the recent sophisticated shell model calculation [29], [43], the result is not in contradiction to the predictions of Refs.[13], [14], [15], however, additional investigations are necessary, especially with independent observables.

(2) The polarization observables for the $^{15}N(\mathbf{p}, \alpha_0)^{12}C$ reaction provide a favourable way to determine the PNC matrix elements. The energy anomaly in the PNC analyzing powers (A_L and A_b) is magnified by nuclear structure effects in addition to the 51 keV energy difference between the levels involved. The magnification arises from coherent contributions of proton and α-channels. The quantity $C_{L(b)}$ describes the ratio between the PC-T-matrix contribution to the PNC analyzing powers and the (unpolarized) cross section for the (p, α) reaction (see Ref.[34]). The value of this ratio is about 0.1 in the resonance region, being a measure for the coherence effect. The width of the 2^-1 resonance level is very small (1.6 keV) and acts as an enhancement factor, too. The ratio $\frac{\Gamma_p^{2^-}}{\Gamma_p^{2^+}}$ has a value 3.4 and is another enhancement factor, as pointed out in Ref.[55] (similar ratios of unnatural-to-natural parity level widths are of the order of 10^{-2} (see, e.g., Refs.[64]).

(3) The cross section for the $^{15}N(p, \alpha_0)^{12}C$-case is maximal at backward angles [126]. Moreover, the normal PC analyzing power is negligible small [126] in this energy region for large scattering angles, which is a favourable situation for measurement. Furthermore, the α-channel can be studied more precisely than it is, e.g., the case of PNC elastic scattering (target impurities, systematic asymmetries due to energy modulations and transverse polarization gradients [56], reduced number of α-channels, etc.).

(4) The PNC α_0-transition can be studied via the $^{15}N(\mathbf{p}, \alpha_0)^{12}C$ resonance reaction with two polarization observables, namely the PNC longitudinal and PNC transverse analyzing powers A_L and A_b. Information about the PNC matrix element can be obtained independently from the excitation energy of each observable. Up to now only the case of the $^{19}F(\mathbf{p}, \alpha_0)^{16}O$ reaction has been studied experimentally [31], [32], [33] giving an upper limit [31] of the corresponding PNC asymmetry.

(5) The theoretical models, included in the OXBASH code, are reasonably good (see Ref.[34], [35]) for the levels of the mentioned 2^-, 2^+-doublet, since the even-even nucleus is an often used candidate being well described by such realistic models. Especially, the (first) excited $J^\pi = 2^-1$ state can reliably be reproduced.

These conclusions are based on the following investigations. Because of the small proton energy the angular momentum can be restricted to $l \leq 2$. Together with the spins and parities of the involved nuclei the following four PC transition amplitudes are allowed:

$$t_1 = T_{bg} = T^{0^+}_{\alpha 00, p\,11}; \qquad t_2 = T^{1^-}_{\alpha 10, p\,01};$$
$$t_3 = T^{1^-}_{\alpha 10, p\,21}; \qquad t_4 = T^{2^+}_{\alpha 20, p\,11}. \tag{31}$$

Two PNC transition amplitudes are taken into account:

$$T_1 = T^{2^{+,-}}_{\alpha 20, p\,20}; \qquad T_2 = T^{2^{+,-}}_{\alpha 20, p\,21}. \tag{32}$$

The general form of the PC resonance T-matrix elements is the following:

$$T^{J^\pi}_{\beta ls, \beta_1 l_1 s_1} = \frac{i \exp(i\xi_{\beta ls}) \sqrt{\Gamma^{J^\pi}_{\beta ls}} \sqrt{\Gamma^{J^\pi}_{\beta_1 l_1 s_1}} \exp(i\xi_{\beta_1 l_1 s_1})}{E - E^{J^\pi} + i/2\,\Gamma^{J^\pi}} \tag{33}$$

while the PNC T-matrix elements have the following expression:

$$T^{J^{\pi,-\pi}}_{\beta ls, \beta_1 l_1 s_1} =$$
$$= \frac{i \exp(i\xi_{\beta ls, \beta_1 l_1 s_1}) \sqrt{\Gamma^{J^{-\pi}}_{\beta ls}} \langle J^{-\pi} | H_{PNC} | J^\pi \rangle \sqrt{\Gamma^{J^\pi}_{\beta_1 l_1 s_1}} \exp(i\xi_{\beta_1 l_1 s_1})}{(E - E^{J^{-\pi}} + \frac{i}{2}\Gamma^{J^{-\pi}})(E - E^{J^\pi} + \frac{i}{2}\Gamma^{J^\pi})} \tag{34}$$

$\beta(\beta_1)$ stands for $\alpha(p)$, $\xi_{\alpha(p)ls}$, E^{J^π} and Γ^{J^π} stand for the $\alpha(p)$-channel phases, resonance energies and total resonance widths, respectively. E is the proton energy in the compound system. The quantities $\sqrt{\Gamma^{J^\pi}_{\alpha(p)ls}}$ are taken from experiments [64], [126] if available; otherwise they are expressed in terms of the OXBASH spectroscopic amplitudes [63], geometrical coefficients and s.p. channel widths.

The calculations within the OXBASH code gave the following results:

$$\left|\frac{\sqrt{\Gamma^{1^-}_{p21}}}{\sqrt{\Gamma^{1^-}_{p01}}}\right| = 2\cdot 10^{-3}; \qquad \Gamma^{1^-}_{p01} \simeq \Gamma^{1^-}_{p}\,(\exp) = 100\ \text{keV}; \tag{35}$$

$$\left|\frac{\sqrt{\Gamma^{2^-}_{p20}}}{\sqrt{\Gamma^{2^-}_{p21}}}\right| = 1; \qquad \Gamma^{2^-}_{p20} = \Gamma^{2^-}_{p21} = \frac{1}{2}\Gamma^{2^-}_{p}\,(\exp) = 0.495\ \text{keV}; \tag{36}$$

$$\Gamma^{2^+}_{p11} = \Gamma^{2^+}_{p}\,(\exp) = 3.4\ \text{keV}. \tag{37}$$

It turns out that $T_1 = T_2$. Contributions from the spin-orbit potential to the proton channel phases and spectroscopic amplitudes have been neglected due to the low proton energy ($E_p \simeq 900$ keV).

In the following we discuss the degree of accuracy of the shell model calculations within the available OXBASH code in order to substantiate the opinion that, the experimental results on PNC analyzing powers of the $^{15}\text{N}(\mathbf{p}, \alpha_0)^{12}\text{C}$ resonance reaction with $E_p \simeq 0.898$ MeV can be analysed free from nuclear structure uncertainties.

In order to predict the magnitude of the effect and to check the feasability of an experiment to measure A_L and/or A_b around the resonance energy of the first excited 2^-1 state in ^{16}O we calculated the

$$\langle 2^-1,\ 12.9686\ \text{MeV}\,|\,H_{PNC}\,|\,2^+0,\ 13.020\ \text{MeV}\rangle \tag{38}$$

matrix element using the OXBASH code in the Michigan State University version [63], which includes different model spaces and different residual effective two nucleon interactions.

Two different model spaces have been used: the ZBM and PSD model spaces (see section 3). In order to maintain the matrix dimensions at a non-prohibited level, the nucleons have been considered to be frozen in the $1p_{3/2}$ orbit; thus a fixed $(1s_{1/2})^4(1p_{3/2})^8$ configuration is assumed in all cases. It turns out that at least four particle-four hole calculations are needed [16], [127], [128] in order to describe the 2^+ states in ^{16}O.

Five different residual interactions have been used in ZBM model space: ZBM I, ZBM II, REWIL, ZWMO and ZWM. Two different combinations of interactions have been taken into account in the PSD model space: PSDMK, PSDMWK. While the centre of mass spuriosity is small in the ZBM model space, the number of spurious components is high in the PSD space, but the degree of spuriosity of every component is small. In PSDMK + CM and

PSDMWK+ CM the contributions of spurious components were eliminated with a procedure analysed in Ref.[118].

The one-body part (see eq.15) of the PNC matrix element turns out to be the dominant in all described cases.

The TBME have been calculated with harmonic oscillator wave functions ($\hbar\omega = 14$ MeV is appropriate for $A = 16$) [25].

The short range correlations (SRC) of the shell model wave function were implemented by multiplying the radial two-body wave function by a Jastrow factor (see section 3). In Table 2 of Ref.[35] are presented the nuclear structure parts of the PNC matrix element, with and without SRC included and separately the single and two particle contributions.

Moreover, recently [129], [130] the experimental measurements showed a relatively strong isospin mixing of the 2^-1, $E_x = 12.9686$ MeV level with the 2^-0, $E_x = 12.53$ MeV level in $^{16}O^*$. In Ref.[35] it was shown that the isospin impurity of the $2^- T = 0$, $E_x = 12.53$ MeV into the $2^- T = 1$, $E_x = 12.9686$ MeV level does not change significantly the results of Ref.[34], i.e., the PNC analyzing powers increase their values with $\approx 30\%$ if taking the sign of the isospin impurity as given in eq.(1) of Ref.[35].

In these calculations the standard form for H_{PNC} has been used (see section 2) with the weak coupling constants given in Tables 2 and 3. The strong coupling constants are summarized in the last four columns of Table 2 from Ref.[15]. The calculated PNC matrix elements for different weak interaction models and different shell model residual interactions are shown in Table 4. As can be seen, the results for different interactions agree within a factor of 2.5 and no large suppression appears when the model space is enlarged. The ρ and ω exchange contributions add coherently to the total matrix element in every case [34], [35]. The contributions from heavy mesons do not exceed 25% for the DDH, AH and DZ cases but increase to 50% in the KM model, reducing the contribution of pion exchange. If this model is taken at face value, the chance to observe a trace of $h_\pi^{(1)}$ is considerably decreased.

Considering the present discrepancies between the DDH-values [13] and the KM [15] results, the conservative choice of the matrix element $\langle 2^-1 | H_{PNC} | 2^+0 \rangle \simeq 0.1$ eV is consistent with the DZ [14] — model and is also supported by $\Delta T = 1$ PNC experiments [16]. In this case 75% of the value arises from pion exchange. The contribution of the new class of diagrams in the PNC single particle Hamiltonian, recently proposed by Caprini and Micu [96], vanishes for the proposed matrix element.

It is essential to compare the predictions of the above theoretical model with the experimental results for the cross section and the (regular) analyzing

Table 4. (M_{PNC} PMD1 ^{16}O)

Inter-actions	DDH			AH			DZ		
	V_π	$V_{\rho(\omega)}$	V_{tot}^{DDH}	V_π	$V_{\rho(\omega)}$	V_{tot}^{AH}	V_π	$V_{\rho(\omega)}$	V_{tot}^{DZ}
ZBM I	−0.287	−0.016	−0.303	−0.138	−0.028	−0.166	−0.086	−0.021	−0.107
ZBM II	0.660	0.036	0.696	0.306	0.061	0.367	0.189	0.047	0.236
REWIL	0.332	0.017	0.349	0.154	0.290	0.183	0.095	0.023	0.118
ZWM	−0.709	−0.037	−0.746	−0.328	−0.064	−0.392	−0.204	−0.050	−0.254
PSDMK	−0.381	−0.014	−0.395	−0.176	−0.029	−0.205	−0.109	−0.022	−0.131
PSDMK + + CM	0.304	0.021	0.325	0.141	0.041	0.182	0.087	0.031	0.118
PSDMWK	0.437	0.020	0.457	0.202	0.040	0.242	0.125	0.031	0.156
PSDMWK + + CM	0.423	0.025	0.448	0.196	0.049	0.245	0.122	0.037	0.159

The PNC matrix element for the PMD1 in the ^{16}O calculated within different weak and strong interactions. The abbreviations are discussed in the text.

power for the $^{15}N(p, \alpha)^{12}C$ reaction. The resonance parameters for the used PC T-matrices, are taken from the latest compilation [64]. The proton phases ξ_{pls} have been calculated within a folding procedure, using a realistic M3Y interaction [44]. The results are very close to the Coulomb phases. The α-channel phases and the background PC 0^+0 T-matrix element $t_1 = t \exp(i(\alpha))$ have been fitted to reproduce the Legendre polynomial coefficients for the cross section and the PC analyzing power of Pepper and Brown [126]. The expansion coefficients extracted from experiment and from the present investigation (see Ref.[34]) shows the quality of the theoretical treatment. The calculation of the PNC analyzing powers A_L and A_b has been performed with the same parameters. The PNC analyzing power shows a dispersionlike energy behaviour around the resonance energy, the form depending on the phase difference of the contributing matrix element. However, the difference between the maximum and the minimum is equal to the quantity $D_{L(b)}$ defined in eq.(26). It is a very important fact that this quantity does neither depend on the phase φ_{PNC} nor on the PC phase $\varphi_{L(b)}$ of $C_{L(b)}$.

In Fig.1(a,b,c,d) we show on expanded horizontal scale the predicted size of the quantities relevant for an experiment designed to determine the PNC matrix element by measurement of A_L and/or A_b around the narrow 2^-1

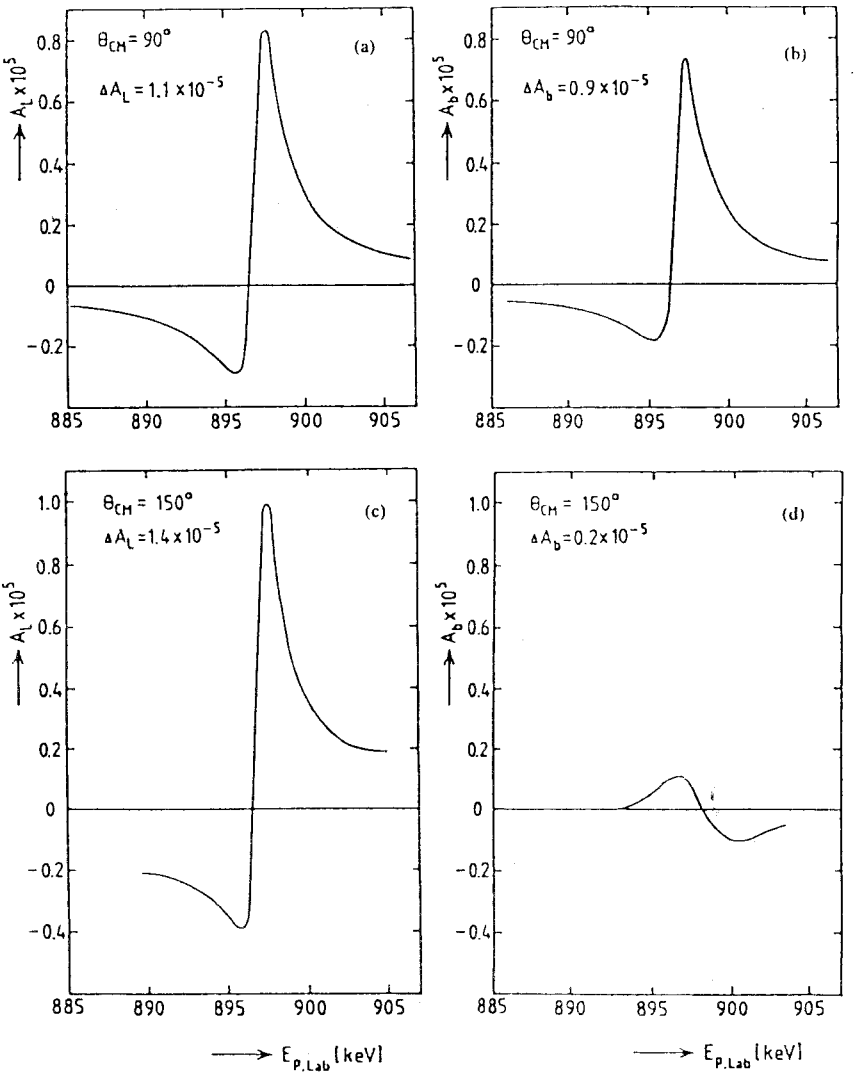

Fig.1 (a, b, c, d). Longitudinal and the irregular transverse analyzing powers of the reaction $^{15}N(p, \alpha_0)^{12}C$ versus proton energy, for $\theta = 90°$ and $150°$ around the proton energy $E_p^{LAB} \approx 0.9$ MeV ($M_{PNC} = 0.1$ eV)

resonance. The information on the modulus of the PNC matrix element can therefore be extracted from $A_{L(b)}$ measurements.

On the base of these predictions an experimental proposal to measure the PNC analyzing powers A_L (and A_b) in the $^{15}N(\mathbf{p}, \alpha_0)^{12}C$ reaction is sketched in the following. At backward scattering angles the (PC) analyzing power A_n is very small or even zero [126], whereas the cross section is maximal in the relevant energy region around $E_{res}(2^-1) \approx E_p = 898$ keV. This situation is favourable for PNC asymmetry measurements because several PS asymmetry effects, superimposed on the PNC observables, are small if A_n is small. Moreover, this advantage coincides with the maximum of the predicted PNC interference effect in A_L (e.g. $\Delta A_L(\theta_{CM} = 160°) = 2.6 \cdot 10^{-5}$). Although the size of the quantity A_b is smaller than A_L in many experimental cases, it has a comparable size near $\theta = 90°$. However, at this angle the differential cross section appears to be smaller as compared to its magnitude at large angles [34]. Therefore, and because of the solid angle restriction in the A_b measurement (detectors only in one reaction plane) the observable A_L is the more favourable one for the realization of a PNC experiment.

The small width of the 2^--level at $E_p = 898$ keV requires a thin ^{15}N target ($\Delta E \leq 1$ keV for $E_p = 898$ keV), e.g., realized by implanting ^{15}N-ions in the surface of a Ti-backing or preparing a thin Ti ^{15}N-target layer, as has been used in Ref.[36]. Another possibility is the use of a ^{15}N-gas target. It has the advantage, that the energy loss in the target gas can be adjusted in a way that one is able to measure five different energy points around the resonance energy simultaneously. In this case up to 20 Si surface barrier detectors (or parallel plate avalanche counters) can be installed in five rings around a long target gas tube, e.g., at $\theta_{Lab} = (135 \pm 24)°$ or $\theta_{Lab} = (90 \pm 24)°$, as well as at lower energies with large solid angles ($0.4 \leq \Omega \leq 0.6$ sr). The azimuthal angles $\varphi = 0°$, 90°, 180°, and 270° have been chosen to be sensitive for (on line) monitoring of spurious asymmetries caused by residual transverse polarization components of the beam. The scattered particles leave the gas tube through aluminum foils (12 μm – 15 μm), which are used in front of the detectors in order to stop elastically scattered protons and low energy α_1 particles from excited ^{12}C states, providing background free α_0 spectra. The reaction energy can be adjusted precisely by detecting the γ-rays from the $^{15}N(\mathbf{p}, \gamma)^{16}O^*$ reaction. These spectra serve at the same time as a monitor for detecting carbon built-up products on the entrance foil of the gas tube, to correct for this time dependent additional energy loss of the proton beam. The entrance foil is a selfsupporting carbon layer of the thickness less than 60 nm in order to minimize the energy loss and

Table 5. (M_{PNC} PMD2 ^{16}O)

Interactions	KM			DDH		
	V_π	$V_{\rho(\omega)}$	V_{tot}^{KM}	V_π	$V_{\rho(\omega)}$	V_{tot}^{DDH}
ZBMI	−0.006	−0.012	−0.019	−0.168	−0.012	−0.181
ZBMO	−0.031	−0.033	−0.064	−0.748	−0.030	−0.778
ZWM	−0.024	−0.019	−0.043	−0.574	−0.030	−0.604
REWIL	−0.011	−0.006	−0.018	−0.285	−0.005	−0.291
ZBMII	−0.002	+0.001	−0.002	−0.064	+0.001	−0.064
Interactions	AH			DZ		
	V_π	$V_{\rho(\omega)}$	V_{tot}^{AH}	V_π	$V_{\rho(\omega)}$	V_{tot}^{DZ}
ZBMI	−0.070	−0.024	−0.094	−0.044	−0.018	−0.062
ZBMO	−0.344	−0.059	−0.404	−0.214	−0.047	−0.261
ZWM	−0.264	−0.034	−0.298	−0.164	−0.027	−0.019
REWIL	−0.131	−0.011	−0.142	−0.081	−0.009	−0.090
ZBMII	−0.030	+0.001	−0.028	−0.018	+0.001	−0.018

The PNC matrix element for the PMD2 in the ^{16}O calculated within different weak and strong interactions. The abbreviations are discussed in the text.

straggling of the proton beam. This is essential because of the small resonance width of the 2^- level. Selecting an energy resolution of the polarized proton beam of $\approx \pm 0.6$ keV provided by two narrow feedback slit systems and adjusting the target gas pressure to ≈ 1.3 mbar, the measurement can be performed at five energies simultaneously within the interval $E_{res} - 3/2\Gamma \leq E_{res} \leq E_{res} + 3/2\Gamma$. With an experimental set-up of this type a statistical accuracy of $\approx 0.3 \cdot 10^{-5}$ and $\approx 0.5 \cdot 10^{-5}$ will be reached for $A_L(135 \pm 24)°$ and $A_L(90 \pm 24)°$, respectively, after 48 $\mu A \cdot d$ of integrated beam charge, if the helicity of the proton beam is switched between $\pm P_z$ with $P_z \geq 0.70$. In order to achieve a sufficient experimental accuracy the experiment requires a proton beam with high intensity, polarization, and energy resolution. Due to the low target gas pressure and the high energy resolution restricted by the small resonance width, it is advantageous to improve the experimental set-up by use of a differentially pumped gas target without entrance foil.

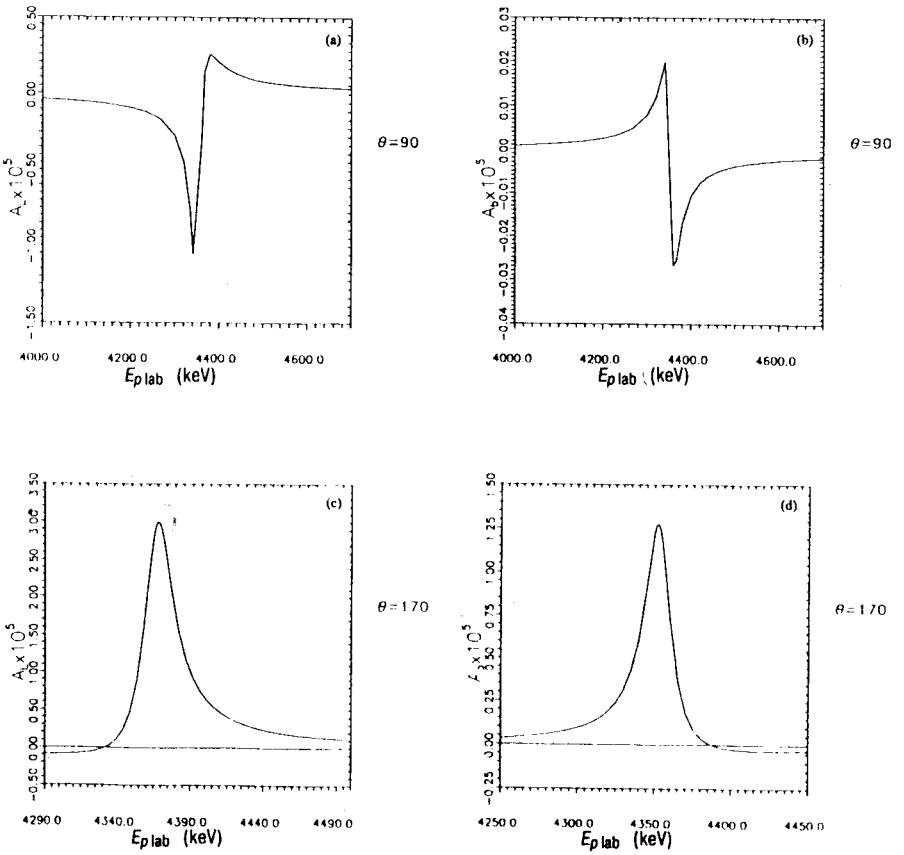

Fig.2 (a, b, c, d). Longitudinal analyzing power of the reaction $^{15}N(p, \alpha_0)^{12}C$ versus proton energy, for $\theta = 90°$ and 170° around the proton energy $E_p^{LAB} \approx 4.35$ MeV (M_{PNC} = = 0.4 eV)

The investigations concerning the second isovector PMD in ^{16}O have been performed in the Ref. [42]. Within the shell model code (OXBASH) with ZBM model space and different interactions (see Table 5) we calculated the PNC matrix element and PNC analyzing powers (A_L and A_b) . The average value for the PNC matrix element is 0.4 eV. The maximum in the energy anomaly of the PNC analyzing powers (A_L and A_b) we got to be some units above the 10^{-5}, value considered to be in agreement to the last measurements [56], [19] (see Fig.2(a,b,c,d).

5. GAMMA ASYMMETRIES

The degree of circular polarization (helicity asymmetry) of the emitted γ-rays is given (see Ref.[133] chapter 9, §3 eq.(9.38)) by a sum of parity non-conserving (PNC) and parity conserving (PC) contributions:

$$P_\gamma(\cos\theta) \equiv \frac{W_{\text{right}}(\theta) - W_{\text{left}}(\theta)}{W_{\text{right}}(\theta) + W_{\text{left}}(\theta)} =$$

$$= \Big(\sum_{LL'\nu} B_\nu(I)\, F_\nu(LL'I'I)\, [\delta_{L+L'+\nu,\,\text{odd}}(m_L^* m_{L'} + e_L^* e_{L'}) +$$

$$+ \delta_{L+L'+\nu,\,\text{even}}(m_L^* e_{L'} + e_L^* m_{L'})]\, P_\nu(\cos\theta)\Big) \times$$

$$\times \Big(\sum_{LL'\nu} B_\nu(I)\, F_\nu(LL'I'I)\, [\delta_{L+L'+\nu,\,\text{even}}\,(m_L^* m_{L'} + e_L^* e_{L'}) +$$

$$+ \delta_{L+L'+\nu,\,\text{odd}}(m_L^* e_{L'} + e_L^* m_{L'})]\, P_\nu(\cos\theta)\Big)^{-1} =$$

$$= (P_\gamma)_0\, R_\gamma^{PNC}(\cos\theta) + R_\gamma^{PC}(\cos\theta), \tag{39}$$

and the circular polarizations for unpolarized initial nucleus with zero and finite mixing ratios [134], respectively are:

$$(P_\gamma)_0 = 2\,\frac{M_{PNC}}{\Delta E}\sqrt{\frac{b_+\tau_-}{b_-\tau_+}\left(\frac{E_\gamma^-}{E_\gamma^+}\right)^3}, \tag{40}$$

and

$$(P_\gamma)_{un} = (P_\gamma)_0\sqrt{\frac{1+\delta_-^2}{1+\delta_+^2}}. \tag{41}$$

R_γ^{PNC} is a multiplier due to the existence of the orientation of the nucleus in the initial excited state when the mixing ratios do not vanish, which for instance in the case of $A = 36$ gamma transitions reads [46], [47], [30]:

$$R_\gamma^{PNC}(\cos\theta) = \sqrt{\frac{1+\delta_-^2}{1+\delta_+^2}}\,\Big\{\sum_{\nu=0,2,4} P_\nu(\cos\theta)\, B_\nu(2)\, [F_\nu(1122) + F_\nu(2222)\,\delta_+\delta_+ +$$

$$+ F_\nu(1222)\,(\delta_- + \delta_+)]\Big\}\,\Big\{\sum_{\nu=0,2,4} P_\nu(\cos\theta)\, B_\nu(2)\, [F_\nu(1122) +$$

$$+ F_\nu(2222)\,\delta_-^2 + 2F_\nu(1222)\,\delta_-]\Big\}^{-1}, \tag{42}$$

where the F_ν coefficients are defined by

$$F_\nu(LL'I'I) = (-1)^{I'+3I-1}[(2I+1)(2L+1)(2L'+1)]^{1/2},$$
$$C(LL'\nu;\ 1-10)\ W(LL'II;\ \nu I'), \tag{43}$$

C is the Clebsch–Gordan coefficient $C(J_1J_2J_3;\ M_1M_2M_3)$ and W is the Racah coefficient. The parity conserving (PC) γ-asymmetry is given by [133]:

$$R_\gamma^{PC}(\cos\theta) = \{\sum_{\nu=1,3} P_\nu(\cos\theta)\, B_\nu(2)[F_\nu(1122) + F_\nu(2222)\delta_-^2 + 2F_\nu(1222)\delta_-]\}\times$$
$$\times\{\sum_{\nu=0,2,4} P_\nu(\cos\theta)\, B_\nu(2)[F_\nu(1122) + F_\nu(2222)\delta_-^2 + 2F_\nu(1222)\delta_-]\}^{-1}, \tag{44}$$

where

$$B_\nu(2) = \sum_M (2\nu+1)^{1/2}\, C(2\nu 2;\ M0M)\, p(M), \tag{45}$$

$p(M)$ is the polarization fraction on the M-state, which determines the degree of the orientation of the nucleus.

In order to measure a PNC effect one must find situations for which the R_γ^{PC} part in eq.(40) vanishes. Two particular cases have this property: i) The case of an initially unpolarized nucleus for which $B_0(2) = 1$, $B_{\nu\neq 0}(2) = 0$ and $F_0(LL'22) = \delta_{LL'}$. In this particularly simple case P_γ reduces to the well-known expression of the circular polarization, $(P_\gamma)_{un}$. ii.) One may prepare a polarized state by choosing $p(M) = \delta_{M0}$ for which $B_{\nu=1,3}(2) = 0$ and R_γ^{PC} part vanishes.

Another observable which measures a PNC effect is the forward-backward asymmetry of the emitted gamma rays by polarized nuclei

$$A_\gamma(\theta) \equiv \frac{W(\theta) - W(\pi-\theta)}{W(\theta) + W(\pi-\theta)}. \tag{46}$$

This observable has been successfully used in the ^{19}F case [18], [19] in order to avoid the small efficiency of the Compton polarimeters when one measures the degree of circular polarization. If the mixing ratios are small (δ_+, $\delta_- \ll 1$) one can show that [39]

$$A_\gamma(\theta) \simeq (P_\gamma)_0\, R_\gamma^{PC}(\cos\theta). \tag{47}$$

The angular distribution described by this formula has a maximum for $\theta = 0°$ [39]. It has the advantage that the parity conserving (PC) cicrcular pola-

rization, $R_\gamma^{PC}(\theta)$, can be measured experimentally. For all these cases the $(P_\gamma)_0$ quantity essentially describes the PNC effect. In all the above formulae θ represents the angle between the emitted photon and the axis of polarization (if any).

5.1. Parity Mixed Doublets in ^{18}F. In the excitation spectrum [64] of the ^{18}F nucleus there are two PMD's (see Table 1): one lying at 1.0 MeV ($\Delta E \approx 40$ KeV) and another one lying at 6.8 MeV ($\Delta E \approx 4$ KeV) excitation energy. The difference between the two PMD's is that the PMD1 is of the isovector type and it can be investigated via the circular polarization of the γ-rays, while the PMD2 cannot be interpreted yet, whether it is of the isoscalar or of the isovector type, because the isospins are not experimentally known, however, it is a very favorable ($F = 130000$, see Table 1) case for studying the structure of the weak hadron-hadron interaction via the (**p**, p) resonance scattering or (**p**, α) resonance reaction.

We want to discuss the first PMD case in somewhat more detail, since it has been the object of considerable experimental and theoretical work. Let us denote the upper state (1.08054 MeV) (see Table 1) by $|a\rangle$ and the lower one (1.041155 MeV) by $|b\rangle$. The γ-decay of the state $|a\rangle$ to the ground state ($J^\pi T = 1^+0$) includes a parity conserving (PC) E1 transition and a PNC M1 transition. The circular polarization can be expressed as follows:

$$P_\gamma = 2f \frac{M_{PNC}}{\Delta E}, \tag{48}$$

where the ratio f of the reduced matrix elements for the regular decays of the members of the doublet can be deduced (apart from the sign) from the known lifetimes [64] and energies

$$f = \frac{m_1}{e_1} = \sqrt{\frac{E_a^3 \tau_a}{E_b^3 \tau_b}} \approx 112. \tag{49}$$

The PMD lifetimes are in the relation: $\tau_a(27.5 \pm 1.9\, ps) >> \tau_b(2.55 \pm 0.45\, fs)$, because isospin selection rules forbid the E1 ($\Delta T = 0$) transition, but not the M1 ($\Delta T = 1$) transition. The circular polarization is, therefore, two orders of magnitude larger than the PNC admixture coefficient $\frac{M_{PNC}}{\Delta E}$. This is a good example of amplififcation of the PNC effect, due to the nuclear structure. The M1 transition from the state $|b\rangle$ to the ground state is one of the strongest known M1 transition ($10.3 \pm 1.5 W.u.$), which further justifies the two-level mixing approximation.

The experimental results are:

Caltech – Seattle [49]	1979	$P_\gamma = (-\ 0.7 \pm 2.0)\cdot 10^{-3}$
Firenze [52]	1980	$P_\gamma = (-\ 0.4 \pm 3.0)\cdot 10^{-3}$
Mainz [53]	1982	$P_\gamma = (-\ 1.0 \pm 1.8)\cdot 10^{-3}$
Bini [51]	1982	$P_\gamma = (0.2 \pm 0.6)\cdot 10^{-3}$
Queens Univ. [50]	1982	$P_\gamma = (0.15 \pm 0.55)\cdot 10^{-3}$

If one takes into account the analyzing power ($\simeq 0.02$) of the Compton polarimeters, this would require a precision $\simeq 1.2\cdot 10^{-5}$ in the counting asymmetry and it might be difficult to maintain the systematic errors lower than this limit. The real value of the circular polarization above mentioned could be some units above 10^{-5} if considering the chiral-soliton approach [15] and, hence, difficult to be exactly measured. This PMD1 case in ^{18}F could be considered a good example for the importance of the PNC matrix element given by the nuclear model calculations in the first predictions of favourable cases. The theoretical value of 0.37 eV [16] comes out to be too large. More sophisticated shell model calculations [43] show a decrease of the value of PNC matrix element with the increase of the number of valence orbitals, thus in agreement with experimental suggestions, however no convergence seems to appear.

5.2. Parity Mixed Doublets in ^{19}F. We consider, however, the only excellent experiments in light nuclei, that concerns the asymmetry A_γ in the 110 KeV γ-ray emission of ^{19}F with respect to the direction of the spin of $\left(\frac{1}{2}\right)^-$-110 KeV state, which is produced with large polarization by the reaction ^{22}Ne(p, α)^{19}F. In the particular case of $\left(\frac{1}{2}\right)^- \rightarrow \left(\frac{1}{2}\right)^+$ transition, $A_\gamma = A_\gamma^{(1)}\, p\left(\left(\frac{1}{2}\right)^-\right)$, where $p\left(\left(\frac{1}{2}\right)^-\right)$ is the polarization fraction of the parent state and the asymmetry $A_\gamma^{(1)}$ for total polarization has the same numerical value as the circular polarization P_γ.

The experimental results are:

Seattle [18]	1982	$A_\gamma^{(1)} = (-\ 8.5 \pm 2.6)\cdot 10^{-5}$
Zuerich [19]	1982	$A_\gamma^{(1)} = (-\ 4.5 \pm 3.6)\cdot 10^{-5}$

The theoretical value of circular polarization can be obtained from the following formula:

$$P_\gamma = 2\,\frac{M_{PNC}}{\Delta E}\,\frac{\mu_1^{1/2^-} - \mu_1^{1/2^+}}{\langle \left(\frac{1}{2}\right)^- | E_1 | \left(\frac{1}{2}\right)^+ \rangle} \tag{50}$$

in which the reduced matrix element of the irregular M1-transition depends on the difference of static magnetic-dipole moments in the ground and the first excited state of ^{19}F. The former is known, $\mu\left(\left(\frac{1}{2}\right)^-\right) = 2.628$ n.m. [64], while the latter can be calculated with reasonable accuracy [18], [24], [135] and comes out to be small, $\mu\left(\left(\frac{1}{2}\right)^+\right) = -0.2$ n.m. From the lifetime $\tau = (853 \pm 10)$ ps of the 110 KeV level [64] we can estimate the E1 matrix element and the small enhancement factor comes out to be $f \simeq 11$. The circular polarization then can be obtained to be equal to $(-8.9 \pm 1.6)\cdot 10^{-5}$ if using $M_{PNC} = 0.46$ eV [16], quite in agreement with the experiment.

5.3. Parity Mixed Doublet in ^{21}Ne. One of the best supports for the DDH «best» values comes from the study of the parity violation in the transition: $\frac{1}{2}^-, T = \frac{1}{2}$ (2.789 MeV)$\rightarrow \frac{3}{2}^+, T = \frac{1}{2}$ (g.s.) in ^{21}Ne. According to the analysis made by Millener et al. [27] and subsequently by Haxton et al. [24], the effect should be *a priori* determined by the strength of the neutron-nucleus weak force for its largest part. With the DDH «best» values of the meson-nucleon weak coupling constants, this strength is expected to be small, in agreement with the experimental absence of an effect in this process. Said differently, the isoscalar and isovector contributions of the nucleon-nucleus weak force, which add to each other in ^{19}F, would cancel in ^{21}Ne. This, however, supposes a sizeable isovector contribution, which is not seen in ^{18}F at the expected level: something must be wrong.

While the accuracy of estimations of the PNC effects in light nuclei is not as good as originally expected, one has both in ^{18}F and in ^{19}F some check about the relevant nuclear structure by looking at the β-decay of ^{18}Ne and ^{19}Ne, respectively, which involve an operator, $\boldsymbol{\sigma}\cdot\mathbf{p}$, very close to the one determining PNC effects in complex nuclei in the single particle approximation [136]. There is no similar possible check in ^{21}Ne. Only the comparison of the different calculations can provide some information on the reliability of the estimates. While studies by Millener et al. [27] and Haxton et al. [24] qualitatively agree on the

fact that nuclear structure favours the contribution of the PNC neutron-nucleus force, a quite different conclusion is made by Brandenburg et al. [28]. From the comparison of results with different strong interaction models, they concluded that the isovector contribution, whose sign was changing with the model, is strongly sensitive to the description of the nucleus. In the meantime, this isoscalar contribution was changing by more than an order of magnitude. In this paper, we reexamine these claims on the basis of new calculations including the nuclear models they used. Our conclusion is opposite to their. The isovector contribution is well determined in sign, while the isoscalar one is not. In particular this last contribution may be negligible. In such a case the parity nonconservation in the transition: $\frac{1^-}{2}$, $T=\frac{1}{2}$ (2.789 MeV) $\rightarrow \frac{3^+}{2}$, $T=\frac{1}{2}$ (g.s.) in ^{21}Ne, would be a process sensitive to the isovector part of the weak force, like in the transition: 0^-, $T=0$ (1.08 MeV) $\rightarrow 1^+$, $T=0$ (g.s.) in ^{18}F, and the absence of an effect at the expected level in ^{21}Ne could be usefully correlated with that in ^{18}F.

The circular polarization of photons emitted in the transition $\frac{1^-}{2}$, $T=\frac{1}{2}$ (2.789 MeV) $\rightarrow \frac{3^+}{2}$, $T=\frac{1}{2}$ (g.s.) in ^{21}Ne is expected to be dominated by the contribution from the parity admixture of the $\frac{1^-}{2}$, $T=\frac{1}{2}$-state at 2.789 MeV with the $\frac{1^+}{2}$, $T=\frac{1}{2}$-state at 2.796 MeV. The relation of the circular polarization P_γ to the PNC matrix element $\langle \frac{1^-}{2}, T=\frac{1}{2}$ (2.789 MeV) $|H_{PNC}| \frac{1^+}{2}$, $T=\frac{1}{2}$ (2.796 MeV)$\rangle$ is given by:

$$|P_\gamma(2.789 \text{ MeV})| = \left(10.5 \pm \frac{0.7}{2.8}\right) 10^{-2} \text{ eV}^{-1},$$

$$\left|\langle \frac{1^-}{2}, T=\frac{1}{2} (2.789 \text{ MeV}) |H_{PNC}| \frac{1^+}{2}, T=\frac{1}{2} (2.796 \text{ MeV})\rangle\right|. \quad (51)$$

The calculation of the weak matrix element has been performed with the standard PNC potential, arising from the exhcange of π, ρ and ω mesons, together with various descriptions of the effective *NN* interaction.

We present in Table 6 the details of the contributions of the different components of the PNC potential to the PNC matrix element $\langle \frac{1^-}{2}$,

Table 6

Coupling Element	ZBMI	ZWM (Z)	REWIL (F)	ZBMII	Valence Neutron (^{12}C)	Matrix Transition
$M^{(1)}_{0,\pi}$	0.1884	0.1579	0.2310	0.2592	0.733	$(^3S_1-^3P_1)$
	0.2092	0.1657	0.2557	0.2967		
$M^{(1)}_{0,\rho'}$	0.0116	0.0097	0.0142	0.0159	0.0451	$(^3S_1-^3P_1)$
	0.0146	0.0114	0.0174	0.0203		
$M^{(1)}_{1,\rho}$	0.0092	0.0077	0.0113	0.0127	0.0358	$(^3S_1-^3P_1)$
	0.0127	0.0101	0.0151	0.0174		
$M^{(1)}_{2,\rho}$	0.0116	0.0097	0.0142	0.0159	0.0451	$(^1S_0-^3P_0)$
	0.0065	0.0059	0.0123	0.0142		
$M^{(1)}_{3,\rho}$	0.0098	0.0082	0.0120	0.0134	0.0380	$(^1S_0-^3P_0)$
	0.0071	0.0064	0.0120	0.0137		
$M^{(1)}_{1,\omega}$	0.0086	0.0072	0.0106	0.0119	0.0336	$(^3S_1-^3P_1)$
	0.0146	0.0095	0.0142	0.0163		
$M^{(1)}_{2,\omega}$	0.0110	0.0092	0.0135	0.0151	0.0427	$(^1S_0-^3P_0)$
	0.0061	0.0056	0.0116	0.0135		
$M^{(1)}_{3,\omega}$	0.0091	0.0077	0.0112	0.0126	0.0356	$(^1S_0-^3P_0)$
	0.0067	0.0060	0.0112	0.0128		
$M^{(0)}_{4,\rho}$	0.0077	0.0002	−0.0083	−0.0112	−0.0676	$-\frac{3(^1S_0-^3P_0)+3(^3S_1-^1P_1)}{4}$
	0.0153	0.0032	−0.0083	−0.0105		
$M^{(0)}_{5,\rho}$	0.0004	0.0000	−0.0004	−0.0005		$-\frac{3(^1S_0-^3P_0)-3(^3S_1-^1P_1)}{4}$
	0.0045	0.0040	0.0034	0.0041		
$M^{(0)}_{6,\omega}$	0.0024	0.0001	−0.0026	−0.0035	−0.0213	$-\frac{3(^1S_0-^3P_0)-3(^3S_1-^1P_1)}{4}$
	0.0087	0.0047	0.0009	0.0010		
$M^{(0)}_{7,\omega}$	0.0040	0.0001	−0.0042	−0.0057	−0.0346	$-\frac{3(^1S_0-^3P_0)+3(^3S_1-^1P_1)}{4}$
	0.0093	0.0030	−0.0033	−0.0045		

Values of the matrix elements $M^{(\Delta T)}_{k,s}$ for different description of the nucleus (in units of MeV). In the first column, the matrix elements are reminded. The next columns contain results corresponding to models, whose description is reminded in the text. The results corresponding to the oversimplified model, where the states $\frac{1^+}{2}$ and $\frac{1^-}{2}$ are described by one neutron occupying respectively the $2s_{1/2}$ and $1p_{1/2}$ orbits (with a ^{12}C core) are given in the 6th column. Last column gives the dominant character of the transition for the component under consideration. For each component the contribution corresponding to the ^{12}C core is given in the first row, while the second row incorporates the contribution of the valence nucleons.

$T=\frac{1}{2}$ (2.789 MeV)$|H_{PNC}|\ \frac{1^+}{2}, T=\frac{1}{2}$ (2.796 MeV)$\rangle$. To facilitate the comparison, we don't introduce the coupling constants so that what is given represents the raw matrix elements

$$M_{k,s}^{(\Delta T)}=\langle \frac{1^-}{2}, T=\frac{1}{2}\ (2.789\ \text{MeV})\,|f_{k,s}^{(\Delta T)}|\ \frac{1^+}{2}, T=\frac{1}{2}\ (2.796\ \text{MeV})\rangle, \qquad (52)$$

where the operators $f_{k,s}^{(\Delta T)}$ are defined by eqs.(8). For each of them, beside the total contribution, we give the separate contribution of the core presently built by filling its orbits $1s_{1/2}$ and $1p_{3/2}$. It corresponds in the present case to a single particle transition involving nucleons in orbits $1p_{1/2}$ and $2s_{1/2}$. As a benchmark, we also give the result corresponding to a pure case, where the $\frac{1^-}{2}$ and $\frac{1^+}{2}$ states would be considered as made of one neutron moving in the field of an inert core (^{12}C) and occupying respectively the above orbits $1p_{1/2}$ and $2s_{1/2}$. The comparison with full calculations may evidence specific nuclear structure effects such as depopulation of these single particle states, pairing, possible departures to the single particle approximation together with some suppression or enhancement of particular contributions of the weak force. In reporting the results for various strong interaction models, we gave a particular attention to the intrinsic sign of the weak matrix element $\langle\frac{1^-}{2}, T=\frac{1}{2}$ (2.789 MeV)$|H_{PNC}|\ \frac{1^+}{2}, T=\frac{1}{2}$ (2.796 MeV)$\rangle$. Obviously, this sign is not measurable, since it depends on the sign conventions used to describe the states $|\frac{1^-}{2}, T=\frac{1}{2}$ (2.789 MeV)$\rangle$ and $|\frac{1^+}{2}, T=$ $=\frac{1}{2}$ (2.796 MeV)$\rangle$. However, the comparison of signs obtained with different strong interaction models may be relevant and some change may indicate a strong sensitivity to particular features of the nucleus description. We, therefore, carefully examined these results. The task is not *a priori* straightforward. One may imagine, for instance, that the sign of the isovector contribution is not settled, as stated by Brandenburg et al. [28], while the sign of the isoscalar contribution would be well determined, or vice versa. For the strong interaction models used here, we found that the sign of the largest contribution (at the level of the two-body matrix elements) was the same up to a common phase, leaving no doubt as to the origin of a difference in sign is the results coming out from the computer. The results presented in Table 6 have been corrected so that the dominant individual contributions be the same. Differences in sign between

some of these results therefore reflect differences in the physical description of the nucleus.

Due to the short range of the operators entering the H_{PNC} the estimates of their matrix elements are expected to be very sensitive to short range correlations. To take them into account, we introduced in the calculations the correlation function of Miller and Spencer [65], for even as well as for odd parity components (see section 3.1).

The microscopic structure of the nuclear levels of the parity mixed doublet has been obtained by using the OXBASH code in the Michigan State University version [63], which includes different model spaces and different effective two-nucleon interactions.

In these calculations the ZBM model space and the following interactions: ZBMI, ZBMII, ZWM and REWIL have been used (see section 3).

The comparison with the predictions of the PNC single particle model, (columh labeled «valence neutron» in Table 6) shows that the core contribution is suppressed by a factor 3–4 for the isovector part. For some part, this factor arises from the fact that the $\frac{1^+}{2}$-states and $\frac{1^-}{2}$-states are not described by pure configurations with a neutron in $2s_{1/2}$ and $1p_{1/2}$ orbits, respectively. For the other part, it represents a pairing effect, which, for the type of operator considered here, is usually accounted for by a factor, $u_i u_f - v_i v_f$. Indeed, the dominant PNC contribution, due to the transition $2s_{1/2} \longleftrightarrow 1p_{1/2}$ is cancelled for $\simeq$ 20–30% by the similar, but time reversed, transition $1\bar{p}_{1/2} \longleftrightarrow 2\bar{s}_{1/2}$.

The situation is somewhat similar for the isoscalar contribution, but the pairing effect is much more pronounced, since the contribution of the second transition, $1\bar{p}_{1/2} \longleftrightarrow 2\bar{s}_{1/2}$, becomes comparable to the first one, and even larger in some cases, giving rise either to a complete cancellation (ZWM) or to a change in sign in other cases (ZBMI). The relative weight of these two contributions has been retained in classifying the different models in Table 6, those on the left favorising a proton transition, while those on the right rather evidence a neutron transition. In between, there is a possibility of a total absence of the isoscalar contribution (ZWM), the isovector contribution being relatively stable and varying by a factor of 1.5 at most.

The examination of the contribution of the valence nucleons ($1p_{1/2}$, $1d_{5/2}$, $2s_{1/2}$) is also instructive. As all core nucleons generally contribute coherently to the single particle PNC interaction, one might *a priori* expect that they would increase the core contribution. Looking at Table 6 one sees that it is true in many cases, for the transition $^3S_1$–$^3P_1$ as well as for the transition

$^3S_1$–$^1P_1$ (after appropriately separating in this case the contributions arising from the transitions $^3S_1$–$^1P_1$ and $^1S_0$–$^3P_0$ assumed to dominate). This is not so however for the isovector $^1S_0$–$^3P_0$ transition, whose contribution is small (ZBMII) or even destructive (ZBMI). For the isoscalar $^1S_0$–$^3P_0$ transition the situation is much more contrasted (decrease for ZBMII and increase for ZBMI for absolute values), but, algebraically, the effect always one to go in the same direction. Clearly, the results are very sensitive to strong interactions in $^1S_0$ and $^3S_1$ states, whose relative strength in nuclei is not well determined (see some discussions in Ref. [141] and some other references therein). The well-known pairing correlations between like particles tend to support the dominance of the first one, whereas the existence of the deuteron as a bound state in the $^3S_1$-channel indicates that the corresponding force should have the most important role. As for the core contribution, the dependence of the behaviour of the results on the transition can be traced back to specific «pairing» effects and to a more or less destructive interference of the contributions of the single particle transitions $2p_{1/2} - 1s_{1/2}$ and the time reversed one $1\bar{p}_{1/2} - 2\bar{s}_{1/2}$.

The large variation of the isoscalar contribution with the strong interaction model makes it useful to present a few simple pictures which may occur. Checking how much they are realized in actual results is not easy and they are given as guidelines for future research. The first one supposes that the $\frac{1^+}{2}$-state is given by one neutron in the valence orbit $2s_{1/2}$ moving in the field of a core (^{20}Ne), whose $1p_{1/2}$ shell would not be completely filled. In the single particle approximation, the PNC transition from the state $\frac{1^+}{2}$ to the state $\frac{1^-}{2}$ occurs via a transition from the $2s_{1/2}$ neutron orbit to the $1p_{1/2}$ orbit. It is a particle like transition. This picture seems appropriate to describe results obtained with the ZBMII and REWIL models.

The other schematic pictures are inspired by the Nilsson model and supposes some relationship between the parity doublets considered here and the one in ^{19}F, where parity-nonconservation evidences the character of a proton-hole like transition. The parity doublet in ^{21}Ne might be obtained by creating holes in the deformed orbits [220] $\frac{1^+}{2}$ and [101] $\frac{1^-}{2}$ of ^{20}Ne, to which two inert

nucleons in the orbit [221] $\frac{3^+}{2}$ would be added. Two extreme possibilities occur, depending on whether this pair is in $T = 1$ or in $T = 0$ state. The first one, where the hole is coupled to the $T = 1$ pair, so that the total isospin is $T = \frac{1}{2}$, gives rise to a result where the contributions of the neutron and proton single particle PNC interactions are in the ratio 2:1 corresponding to the ratio of isovector and isoscalar contributions, – 1:3. This picture, which apparently underlies results by Millener et al. [27], where the role of the neutron transition is somewhat enhanced (the above ratios are respectively 3.7:1 and – 1:1.73), has no counterpart here. As mentioned above, results for ZBMII, which favour a neutron PNC transition, correspond to a particle transition and not to a hole one as in the Millener et al. [27] calculations. To get it, the sign of the «pairing» effect for the isovector contribution should change as it does for the isoscalar contribution. While the present calculations evidence a well determined sign for the isovector contribution, it may be that the change in sign observed for the contribution of valence nucleons in some cases (isovector transition $^1S_0$–$^3P_0$) is an indication that the picture underlying Millener et al.'s results is not completely absent from the present results.

Some nuclear aspects of the calculations presented here have already been discussed. Further comments may be in order, especially in relation with other works. Apart for the sign of the isovector contribution we mentioned at length above, we essentially agree with the results of Bradenburg et al. [28], whose models *Z* and *F* correspond to models denoted here by ZWM and REWIL. The large sensitivity to the nuclear model of these results for the isoscalar contribution, apparently unnoticed, is further confirmed by the present results for the models ZBMI and ZBMII. Results of Millener et al. [27] were obtained with a single-particle PNC interaction, (const $\boldsymbol{\sigma}\cdot\mathbf{p}$). For many transition involving low energy states, this approximation, possibly corrected for the finite range of the nucleus, has been able to reproduce the essential features of more elaborated calculations involving two-body forces (see for instance Ref.[138] and references therein). It is interesting to notice that the improved calculations by Adelberger et al. [16] for ^{18}F, ^{19}F and ^{21}Ne evidence a single particle transition character,while the description of these nuclei already reveals a complicated structure. In results presented here, the above approximation still works, but to the extent where the core contribution is the dominant one. Compared to ^{19}F however, relatively large departures appear, especially for ZBMI, where the valence nucleon contribution gives an increase in some cases (factor 2 for the component $g_\rho h^0_\rho (1 + \mu_\nu)$, a decrease in other cases (a factor 1.8 for the compo-

nent $g_\rho h^1_\rho\ (1 + \mu_v)$). This is perhaps an indication that ^{21}Ne is in some transition region, making more difficult well defined predictions. A further support to this statement concerns the character of hole transition of Millener et al.'s and Adelberger et al.'s results, which is confirmed here only for the isoscalar contribution (ZBMI and ZWM). Their approach necessarily implies such a structure since they allow for only one hole in the $1p_{1/2}$ shell. The absence of restriction with this respect in present calculations leads to a quite different picture, since the isovector contribution is uniformly of the particle type transition. In view of them, the above approximation appears to be a poor one. This does not mean that the present results are free from criticism. Studies in ^{18}F and ^{19}F show that some suppression of the PNC effect occurs, due to the deformation of the nucleus, which to be accounted for, requires that particles in $1p_{3/2}$, $1d_{3/2}$ and $1f_{5/2}$ shells be active ones (beside the particles in $1p_{1/2}$, $1d_{5/2}$ and $2s_{1/2}$). The possible transitional nucleus character of ^{21}Ne precludes to make a statement as to the precise role of these corrections, but a provisional suppresion factor 3, as in ^{18}F and ^{19}F, sounds quite reasonable. This should be kept in mind when making the comparison with the experiment.

After discussing some features relative to the nucleus description itself, it may be appropriate to consider those related to the weak interaction. Differences between ρ and ω-exchange contributions reflect differences used for meson masses. Their ratio for terms having the same spin-isospin structure is roughly given by the factor $\frac{m_\rho^2}{m_\omega^2}$ ($\simeq 0.965$ here) corrected for the effect of short range correlations, which tend to decrease it. For isoscalar contributions, this feature is more difficult to check, due to a difficult isospin structure. Concerning the short range correlations, one would expect that the difference between contributions of commutator and anticommutator terms in the PNC potential reflects that one for a valence neutron (the column 6 of Table 6) is dominated by *S* and *P NN*-transitions. The suppression of some contributions partly invalidates the argument, especially for those dominated by the $^1S_0$–$^3P_1$ transition, where the *P* to *D* transitions acquire a relatively larger weight. These last transitions are quite sensitive to the longer range description of ρ and ω exchanges, due, for instance, to the coupling of the ρ to the 2π continuum [139]. Their mirror role suggests to forget them at the present stage of the studies of pNC effects. Table 6 can thus be considerably simplified to be expressed in terms of four elementary amplitudes [137]: $\bar{v}_0^0$ and $\bar{v}_1^1$ ($^1S_0$–$^3P_0$, isoscalar and isovector), $\bar{u}$ ($^3S_1$–$^1P_1$, isoscalar) and $\bar{w}$ ($^3S_1$–$^3P_1$, isovector), where:

$$M^2\bar{v}^{0,1} = -(g_\omega h_\omega^{(0,1)} + g_\rho h_\rho^{(0,1)}) \frac{M^2}{4\pi m_\rho^2} 0.23 -$$

$$- (g_\omega h_\omega^{(0,1)}(1+\mu_s) + g_\rho h_\rho^{(0,1)}(1+\mu_v)) \frac{M^2}{4\pi m_\rho^2} 0.27, \tag{53}$$

$$M^2\bar{u} = -(g_\omega h_\omega^{(0)} - 3g_\rho h_\rho^{(0)}) \frac{M^2}{4\pi m_\rho^2} 0.23 -$$

$$- (-g_\omega h_\omega^{(0,1)}(1+\mu_s) + 3g_\rho h_\rho(0,1)(1+\mu_v)) \frac{M^2}{4\pi m_\rho^2} 0.27, \tag{54}$$

$$M^2\bar{w} = -(g_\omega h_\omega^{(1)} + g_\rho h_\rho^{(1)}) \frac{M^2}{4\pi m_\rho^2} 0.23 -$$

$$- g_\rho h_{\rho'}^{(1)} \frac{M^2}{4\pi m_\rho^2} 0.27 + \frac{1}{\sqrt{2}} g_\pi h_\pi^{(1)} \frac{M^2}{4\pi m_\pi^2} 0.11. \tag{55}$$

The factors 0.23, 0.27 and 0.11 incorporate the effect of both the range (important for the π exchange case) and short range correlations. They may be changed according to the model of short range correlations. For simplicity, we neglected the differences in masses between the ρ and ω mesons. In the case of the π exchange, the factor has been partly estimated in nuclear matter and incorporates the contribution of transitions P-D, D-F whose destructive role may be smaller in light nuclei, thus enhancing the π exchange contribution with respect to this estimate by 15—25%. The results are presented in Table 7. The advantage of the above amplitudes is to make quite easy the incorporation in first approximation of new physical inputs dealing with the short range PNC-NN interaction (short range correlations, tensor coupling between the $^3S_1$ and $^3D_1$ components, other meson exchange, hadronic form factor) without redoing all the calculations.

Further simplification is obtained by using the strengths of the proton and neutron PNC forces:

$$X_N^p = M^2 \left(\frac{1}{2}\bar{u} + \frac{3}{2}\bar{v}^0 + \bar{v}^1 + \bar{w} \right), \tag{56}$$

$$X_N^n = M^2 \left(\frac{1}{2}\bar{u} + \frac{3}{2}\bar{v}^0 - \bar{v}^1 - \bar{w} \right). \tag{57}$$

As mentioned previously, these quantities, which have been used in analysing various PNC effects in complex nuclei [137], may not be so good to represent

Table 7

	Kuo (Ref.[72])	ZBMI	ZWM	REWIL	ZBMII	Valence neutron
$M^{2\bar{w}}$		0.174	0.146	0.214	0.240	0.68
		0.228	0.179	0.272	0.316	
$M^{2\bar{v}^1}$		0.179	0.150	0.219	0.246	0.70
		0.114	0.104	0.203	0.234	
$M^{2\bar{u}}$		0.074	0.002	− 0.080	− 0.100	− 0.68
		0.087	− 0.022	− 0.135	− 0.171	
$M^{2\bar{v}^0}$		0.080	0.002	− 0.089	− 0.114	− 0.68
		0.216	0.089	− 0.035	− 0.050	
$\frac{X_N^p - X_N^n}{2}$	− 0.19	0.177	0.148	0.217	0.243	0.69
		0.172	0.141	0.237	0.275	
$\frac{X_N^p + X_N^n}{2}$	0.24	0.077	0.002	− 0.084	− 0.107	− 0.69
		0.151	0.033	− 0.085	− 0.110	
X_N^p	0.02	0.127	0.075	0.066	0.068	0.
		0.161	0.087	0.076	0.082	
X_N^n	0.22	− 0.050	− 0.073	− 0.150	− 0.175	− 0.69
		− 0.010	− 0.054	− 0.161	− 0.192	

Expressions of the matrix element $\langle \frac{1^-}{2}, T = \frac{1}{2} (2.789 \text{ MeV}) | H_{PNC} | \frac{1^+}{2}, T = \frac{1}{2} (2.796 \text{ MeV}) \rangle$ in terms of the S–P transition amplitudes as defined in [137] ($\bar{w}$ for ${}^3S_1 - {}^3P_1$, $\Delta T = 1$; $\bar{v}^1$ for ${}^1S_0 - {}^3P_0$, $\Delta T = 1$; $\bar{u}$ for ${}^3S_1 - {}^3P_1$, $\Delta T = 0$ and $\bar{v}^0$ for ${}^1S_0 - {}^3P_0$, $\Delta T = 0$, as well as in terms of the strengths of the proton- and neutron-nucleus PNC forces (in units of MeV). As in Table 6, the first row corresponds to a ^{12}C closed core, while the second row incorporates the contribution of valence nucleons. The above results obviously imply approximations such as neglecting contributions from P–D transitions.

the PNC effect in ^{21}Ne. They, nevertheless are usefull to catch in a glance the dominant character of some matrix element: neutron or proton transition. Expressions in terms of them are also given in Table 7.

In the comparison with the experiment, we retain the following features evidenced by the estimates. The estimate of the nuclear part of the isovector contribution is rather well determined. The isoscalar one, including its sign, is uncertain and has a weight rather disfavoured compared to the isovector one (see Table 7). From the comparison of similar calculations with β decay in

^{18}F and ^{19}F, an overall suppression by a factor 3 is quite likely, but it should be kept in mind that the nuclear uncertainty may here result in an effect more complicated than such a factor.

The circular polarization of γ emitted in the transition $\frac{1^-}{2}$, $T = \frac{1}{2}$ (2.789 MeV) $\rightarrow \frac{3^+}{2}$, $T = \frac{1}{2}$ (g.s.) in ^{21}Ne has been measured to be [26]:

$$P_\gamma = (0.8 \pm 1.4) \cdot 10^{-3}. \tag{58}$$

The error is large, but in fact it provides an upper limit, which appears to be quite constraining. Combining results of Table 6 with coupling constants given in Table 3 («best» values of DDH and using the relation of P_γ to the PNC matrix element $\langle \frac{1^-}{2}, T = \frac{1}{2}$ (2.789 MeV)$|H_{PNC}|\frac{1^+}{2}, T = \frac{1}{2}$ (2.796 MeV)$\rangle$ indicates that many of the individual contributions exceed the experimental upper limit, or just reach it. Accounting for a possible overestimate by a factor 3 leaves 2 contributions which may be of some relevance: the π-exchange and the isoscalar ρ-exchange ones (respectively $(10\text{–}20)\cdot 10^{-3}$ and $(-5.8)\cdot 10^{-3}$).

While the isovector contribution in P_γ agrees in size (but not necessarily in sign) with that obtained in similar conditions by Adelberger et al. ($12 \cdot 10^{-3}$) the isoscalar one is smaller than their ($-12 \cdot 10^{-3}$). The nice cancellation between the isovector and isoscalar contributions in their results, which made them consistent with the upper limit on P_γ, does not hold anymore.

Examination of the present results shows that the cancellation is not always present (ZBMI) and that, in cases where there is some, the relative ratio of the π- and ρ-exchange contributions expected from DDH «best» values has to be changed significantly. Fixing the isoscalar ρNN coupling at its «best» DDH value, in agreement with observations of PNC effects in *pp* scattering at low energy (15 MeV and 45 MeV), implies that the corresponding πNN coupling constant be reduced by a factor of 3 in order to match the experimental upper bound on P_γ. The resulting value (REWIL, ZBMII), $h_\pi^{(1)} = 0.15 \cdot 10^{-6}$, would be quite compatible with the limit obtained from the upper bound on the PNC effect in the transition $0^-(1.08 \text{ MeV} \rightarrow 1^+$ (g.s.)) in ^{18}F($|h_\pi^1| < 0.15 \cdot 10^{-6}$). Thus, far from supporting the «best» values of DDH, PNC in ^{21}Ne would add to that in ^{18}F to favour a value of $h_\pi^{(1)}$ significantly smaller than the DDH «best» value.

In discussing PNC effects in nuclei, the effect of the tensor force which admixes $^3D_1$ component to the $^3S_1$ state, is generally neglected. Its role is two-fold here and tends to provide further support for lower values of $h_\pi^{(1)}$. In the case of the π-exchange, it leads to an enhancement of the contribution of the $^3S_1$–$^3P_1$ transition, which compensates a large part of the effect of the short range repulsion at short distances [137]. The actual value of $h_\pi^{(1)}$, which may be extracted from the comparison of measurements to a theoretical estimate more elaborate with the above respect, should be accordingly corrected downwards. The above statement is quite general and also applies to conclusions drown from the study of PNC in ^{18}F [16].

The importance of the role of tensor correlations for the ρ-exchange contribution is somewhat specific to some of the present results for ^{21}Ne (REWIL, ZBMII). As seen from Table 7, the isoscalar contribution for those cases is dominated by the $^3S_1$–$^1P_1$transition. Tensor correlations may reduce it by a factor 3–4 (Reid soft-core case), making the total isoscalar contribution smaller. This requires a lower value of the isovector contribution, and therefore a lower value of $h_\pi^{(1)}$, so that the destructive sum of the isoscalar and isovector contributions still matches the upper limit on the circular polarization, P_γ.

At this point, it may be appropriate to remind a few predictions for $h_\pi^{(1)}$. In this order, the DDH approach is quite useful as it provides a general scheme, where many contributions considered in the literature can be accomodated quite easily. Results are given in Table 8 for different values of the factor $K(K = 1, 4, 7)$ defined in Refs. [13], [142], which characterizes strong interaction effects. Partial contributions are also exhibited. They correspond to the sum rule contribution (related in one way or another to the charge current contribution), to the parity volation in the wave function, and to the factorization approximation. Earlier contributions calculated by Weinberg [4] or Gari and Reid [140] would enter in the column indicated by We and Ga, respectively. Later contribution by Dubovik and Zenkin [14], Kaiser and Meissner [15] or Khatsimovsky [62] may be considered as particular cases of DDH expectations. In spite of somewhat different approaches in some cases, they compare well with them. The corresponding contributions in the DDH scheme are underlined in Table 8 (respectively labeled by KM, DZ and Kh). Contributions involving a (colored) strange content are given in the two first columns, the first one correpsonding to the charge current part of the weak interaction.

As seen from Table 8, small values of $h_\pi^{(1)}$ are found for small values of the factor K or/and in absence of strange content in the nucleon. This might repre-

Table 8

		Sum rule $\bar{s}s$..	PNC factorization in the w.f.	
$K = 1$	$h_\pi^{(1)} = f_\pi^c \cdot ($	$1 + 0 - 3.3$	$+ 2.1 + 1.3)$	$= 0.4 \cdot 10^{-7}$
			...K.M.	$= 0.4 \cdot 10^{-7}$
$K = 4$	$h_\pi^{(1)} = f_\pi^c \cdot ($	$1 + 4.6 - 3.5$	$+ 0.1 + 4.3)$	$= 2.5 \cdot 10^{-7}$
			...D.Z.	$= 0.4 \cdot 10^{-7}$
$K = 7$	$h_\pi^{(1)} = f_\pi^c \cdot ($	$1 + 6.0 - 4.3$	$- 0.5 + 7.0)$	$= 3.5 \cdot 10^{-7}$
	$f_\pi^c = 0.38 \cdot 10^{-7}$	We Ga	Kh	

Detailed contributions to the coupling constants $h_\pi^{(1)}$ in the DDH scheme as completed in Ref.[142]. Results are given for different values of the factor K [142], [13] which accounts for the effect of strong interactions [137]. Three types of contributions are included, respectively denoted: sum rule (related to the charge current contribution), PNC in the wave function and factorization. The results which later one should be compared with are denoted by the initials of the authors. Some earlier results by Weinberg [4], Gari and Reid [140] or Khatsimovsky [62] would enter in the column labeled We ($K \to \infty$), Ga ($K = 0$) or Kh, respectively. Contribution by Kaiser and Meissner [15] or Dubovik and Zenkin [14], would enter in the rows labeled KM or DZ respectively. Contribution involving the (colored) strange content are given in the first two columns. The f_π^c factor has the value $f_\pi^c = 0.38 \cdot 10^{-7}$.

sent a great achievement of studies of PNC effects in nuclear forces. However, it is difficult to neglect the strange content of the nucleon at the present time where it appears to play some role in different places [141], or to imagine that strong interaction effects ($K \neq 1$) are totally absent. More probably, the explanation of a low value of $h_\pi^{(1)}$ is totally absent, or is to be found in the incompleteness of estimates. Due to a lack of information and because it was considered a second order effect in gluon exchange, the contribution of an uncoloured strange component in the nucleon has not been incorporated in the estimates by DDH. As noted by [140] such a contribution could be enhanced by the presence of a large overall factor in the effective weak interaction. On the other hand, this effective interaction only contains the dominant terms. Other ones may play some non-negligible role in estimating the coupling constant $h_\pi^{(1)}$.

We reexamined estimates of the circular polarization of γ-rays emitted in the transition $\frac{1^-}{2}$, $T = \frac{1}{2}$ (2.789 MeV) $\to \frac{3^+}{2}$, $T = \frac{1}{2}$ (g.s.) in ^{21}Ne, which

involves the parity admixture of two closed states $\frac{1^-}{2}$, $T = \frac{1}{2}$ (2.789 MeV) and $\frac{1^+}{2}$, $T = \frac{1}{2}$ (2.796 MeV). New estimates have been added to previous ones. From the study a different interpretation of the measurement is suggested. Contrarily to the previous claim by Brandenburg et al. [28], we found that the isovector contribution is well defined in sign, while the isoscalar contribution is not and somewhat disfavoured. This conclusion agrees with the recent result of Ref. [43] based on much larger valence basis. Our conclusion is based on a careful examination of the sign of the dominant individual contribution. Such a procedure allows one to rise the ambiguity as to an overall sign that somewhat comes at random from the computer in calculating the wave functions. The difference with Adelberger et al. [16] appears to be due to the quite understandable restriction of their calculation to one hole at most in the $p_{1/2}$. Qualitatively, it sounds as if the total result would be the sum of two different contributions which, in a deformed single particle basis, would imply the transition $[220]\,\frac{1^+}{2} \rightarrow [101]\,\frac{1^-}{2}$ (dominant in ^{18}F and ^{19}F) and a transition implying the $\frac{1^+}{2}$ orbit $\left([211]\,\frac{1^+}{2} \right)$, such that the PNC matrix element would read as:

$$\langle V_{PNC} \rangle \simeq \beta^2 \left(\frac{X_N^n + X_N^p}{2} + \frac{X_N^n - X_N^p}{2} \right) - \alpha^2 \left(\frac{X_N^n + X_N^p}{2} + \frac{1}{3} \frac{X_N^n - X_N^p}{2} \right). \quad (59)$$

The first contribution would mainly have a particle-type character, while the second one would be a hole-type transition. By varying continuously the ratio of these two contributions, one would go from results similar to Millener et al.'s [27] schematic ones ($\alpha^2 = 1$, $\beta^2 = 0$) to those where a particle type transition would dominate (REWIL, ZBMII) ($\beta^2 > \alpha^2$), passing through the case where the isoscalar contribution would be absent ($\beta^2 = \alpha^2$). This picture is proposed to roughly illustrate present results. The difficulty to perform calculations in extended enough basis to account at the same time for pairing effects (important in the present results) and deformation effects (important in Adelberger et al.'s results), which both tend to reduce PNC transition amplitudes estimated here, invites to take with some caution any definite conclusion.

Present results support an interpretation different from the one where the small PNC effect in ^{21}Ne would arise from a «fine» cancellation of the large isoscalar and isovector contributions as calculated with the «best» DDH values for the weak coupling constants. The relative (or even complete) suppression of the isoscalar contribution necessarily imposes an upper limit on the isovector

contribution and therefore on the πNN coupling constant, $h_\pi^{(1)}$. Although the conclusion cannot be as convincing as in ^{18}F, where some check is possible from the β decay of ^{18}Ne, a similar limit, $h_\pi^{(1)} < 0.15 \cdot 10^{-6}$, is obtained. An even lower limit could be obtained if the isoscalar contribution was shown to be totally absent in the present PNC transition.

While a low value for the $h_\pi^{(1)}$ is quite consistent with DDH expectations, it supposes inputs that are far from what could be considered as best ones at the present time: absence of strange content in the nucleon and absence of strong interaction effects in building the effective quark interaction in our opinion, the explanation for a low value of $h_\pi^{(1)}$ should be rather found in the contributions, which were considered as negligible until now and, in any case, difficult to estimate.

5.4. Parity Mixed Doublet in $A = 36$ Nuclei. There is another pair of PMD's which can be described approximately with the same strong interaction models, one PMD, first proposed by Dumitrescu and Stratan [46] belongs to the ^{36}Cl energy spectrum and another one to that of the ^{36}Ar (see Table 1 and 9 and Ref.[132]). Neglecting in the ^{36}Cl-case the isotensor contribution we are dealing with two dominant contributions of the opposite signs, one isovector and one isoscalar, while the ^{36}Ar-case is a pure isoscalar one. The last two PMD's are analogous to the ^{18}F–^{19}F case. For example the ^{36}Ar PMD can be populated in the ^{39}K(**p**, α)^{36}Ar reaction ($E_p \approx 3.7$ MeV) in analogy with the ^{19}F-case, while the ^{36}Cl PMD can be populated in the ^{39}K(**n**, α)^{36}Cl reaction ($E_n \approx 0.6$ MeV).

The calculations of the PNC matrix element were carried out with the shell-model code OXBASH [63] in the *sd-pf* model space in which the $2s_{1/2}$, $1d_{5/2}$, $1d_{3/2}$, $2p_{1/2}$, $2p_{3/2}$, $1f_{7/2}$ and $1f_{5/2}$ orbitals are active. The truncations we made within this model space were $(1d_{5/2})^{12}(2s_{1/2}–1d_{3/2})^{8}$ for the positive parity states and $(2s1d)^{19}(2p1f)^{1}$ for negative parity states ($(0 + 1)\hbar\omega$ calculations). These truncations are necessary due to the dimension limitations, but we believe that they are realistic. The Brown-Wildenthal interaction [143] was used for the positive parity states and the WBMB interaction [144] was used for the negative parity states. Both interactions have been tested extensively with regards to their reproduction of spectroscopic properties [144], [143]. The caclulation of the PNC matrix element which included both the core (inactive) and active orbitals has been performed as described in Ref.[25].

All the components [13], [16] of the parity nonconserving potential are short range two-body operators. Because the behavior of the shell-model wave

Table 9

Nucleus	^{36}Cl	^{36}Ar
$I_i^{\pi}T_i$, E_i (MeV) → $I_f^{\pi}T_f$, E_f (MeV)	2^+1, 1.959 MeV → 2^+1, g.s.	2^+0, 4.951 MeV → 2^+0, 1.97 MeV
$I_i^{\pi}T_i$, E_i (MeV) → $I_f^{\pi}T_f$, E_f (MeV)	2^-1, 1.951 MeV → 2^+1, g.s.	2^-0, 4.974 MeV → 2^+0, 1.97 MeV
life time (τ_+)	(60 ± 15) fs	≤ 50 fs
life time (τ_-)	(2.6 ± 0.3) ps	(14 ± 5) ps
branching ratio (b_+)	94.4%	15%
branching ratio (b_-)	60%	(4.0 ± 0.9)%
mixing ratio $(\delta_+)_{exp}$	(−. 5.2 ± 0.06) or (− 0.10 ± 0.06) [146]	
mixing ratio $(\delta_+)_{theor}$	− 0.24	0.41
mixing ratio $(\delta_-)_{exp}$	(− 0.10 ± 0.10) [146]	
mixing ratio $(\delta_-)_{theor}$	0.009	
$B(E1)_{exp}$	$1.4 \cdot 10^{-5}$	$0.7 \cdot 10^{-7}$ (if $\delta_- = 0$)
$B(E1)_{theor}$		
$B(M2)_{exp}$	≤ 25	
$B(M2)_{theor}$	2.5	0.24
$B(M1)_{exp}$	0.08 ($\delta_+ = -0.2$); 0.003 ($\delta_+ = -5.2$)	0.6 (if $\delta_+ = 0$)
$B(M1)_{theor}$	0.14	0.0009
$B(E2)_{exp}$	12 ($\delta_+ = -0.2$); 298 ($\delta_+ = -5.2$)	
$B(E2)_{theor}$	30	0.27
M_{PNC}^{DDH} (eV)	− 0.019	0.122
M_{PNC}^{DDH} (eV), $h_\pi^1 = \frac{1}{4}(h_\pi^1)_{DDH}$	− 0.057	0.122
M_{PNC}^{KM}	− 0.023	0.067
f	8.3	32.4
F	2000	2400

Physical quantities and theoretical PNC matrix elements necessary for calculating γ-circular polarizations and asymmetries for the two PMD-cases studied in the $A = 36$ cases (see section 5.4). The experimental data is taken from Ref.[132] unless noted.

functions at small NN distances has to be modified, short range correlations (SRC) were included by multiplying the harmonic oscillator wave functions (with $\hbar\omega = (45 \cdot A^{-1/3}\ \text{MeV} - 25 \cdot A^{-2/3}\ \text{MeV})$ by the Miller and Spencer factor [65]. This procedure is consistent with results obtained by using more elaborate treatments of SRC such as the generalized Bethe–Goldstone approach [66], [67]. The PNC pion exchange matrix is decreased by 30 ÷ 50% as compared with the values of the matrix elements without including SRC, while the ρ(ω) exchange matrix elements are much smaller (by a factor of $\frac{1}{3} \div \frac{1}{6}$).

The calculated by Horoi [47] excitation energies of the first three $2^+T = 0$-levels in ^{36}Ar are 1.927, 4.410 and 7.714 MeV. The first two are in good agreement with experimental levels at 1.970 and 4.440 MeV. The third 2^+0 $E_x = 4.951$ MeV state (the state belonging to the parity doublet) apparently is an intruder in the $2s1d$ ($0\hbar\omega$) configuration. This conclusion is also supported by the suppressed β transition probability [145]. Horoi included the $2\hbar\omega$ configurations in a rather reduced space (the $1d_{5/2}$ orbital is freezed and the $1f_{1/2}$ orbital is not allowed) which we consider adequate for this problem. The $2\hbar\omega$ configurations have been shifted down by 11.5 MeV so that the first 2^+0 state with a dominant $2\hbar\omega$ component (~80%) became the third 2^+0 in the calculated spectrum. The dominant PNC transition is $1d_{3/2}$–$2p_{3/2}$ and the PNC matrix element is 0.122 eV (see Table 1). One must mention that this value is more uncertain as compared with the ^{36}Cl value due to the fact that the third 2^+0 state cannot be described either as a pure $0\hbar\omega$ configuration neither as a pure $2\hbar\omega$ configuration. In the ^{36}Cl case, the positive parity states are in very good agreement with the experiment (e.g., the second 2^+ state has a theoretical energy 2.004 MeV, compared to the experimental value of 1.96 MeV). The theoretical $B(E\lambda)$ and $B(M\lambda)$ and mixing ratios are in relatively good agreement with the experiment (see Table 9), for both cases.

The results (up to a complex phase factor) can be summarized as:

$$M_{PNC}(^{36}\text{Cl}) = (1.094h_\pi^{(1)} - 0.205h_\rho^{(1)} - 0.304h_\omega^{(1)} - 0.027h_{\rho'}^{(1)} + 0.569h_\rho^{(0)} + 0.323h_\omega^{(0)} + 0.015h_\rho^{(2)}) \cdot 10^{-2}\ \text{eV}, \tag{60}$$

and

$$M_{PNC}(^{36}\text{Ar}) = -(0.995h_\rho^{(0)} + 0.443h_\omega^{(0)}) \cdot 10^{-2}\ \text{eV}. \tag{61}$$

Here $h_{\text{meson}}^{\Delta T}$ should be given in units of 10^{-7} as in Table 2.

6. CONCLUSIONS

The PNC nuclear physics processes determined by the isovector part of the weak hadron-hadron interaction are very important for studies of the neutral currents.

Our understanding of the $\Delta S = 0$ hadronic weak interaction is based on a small collection of high precision experiments (see for review Ref.[16]) in the two-nucleon system and light nuclei, which isolates the weak interaction via its parity nonconserving signature. The experiments have yielded significant but incomplete information on weak meson-nucleon coupling constants, which are in qualitative agreement with the predictions [13], [14] based on the standard model, although the pion coupling ($h_\pi^{(1)}$) is much smaller than expected. Unfortunately the measured observables need a complicate theoretical interpretation and the extraction of the weak meson-nucleon couplings from the experiment is not model independent at present. Due to the generally small values of most of the contributing terms to the PNC matrix elements, PNC dealing with low energy nuclear spectrum should essentially involve the strength of the nucleon-nucleus weak force. As weak interactions do not conserve the isospin, this strength may be characterized by two numbers, relative to the proton and neutron forces, respectively, or equivalently to its isovector and isoscalar components. Moreover, the main contribution coming from the isovector part is assumed to be due to the one pion exchange term (the long range term), while the main contribution coming from the isoscalar part is assumed to be due to one ρ-meson exchange term (the short range term). At present no experiment is possible to invent in order to be sensible to other contributions to the weak hadron-hadron interaction potential. Therefore, in principle two independent experiments should be sufficient for the determination of the above nucleon-nucleus weak forces. Therefore in this work we tried to select pairs of experiments for which one uses more or less the same theoretical treatment. We investigated the possibility to extract from the experiment the necessary information concerning the neutral current contributions to the structure of the weak interactions that violate the parity conservation low. The low energy nuclear physics processes considered here were: the resonance nuclear scattering and reactions induced by polarized protons, emission of polarized gamma rays from oriented and non-oriented nuclei and parity forbidden alpha decay. Some comments on PNC nucleon-nucleon (PNC-*NN*) interaction have been presented. Applications for specific scattering, reaction and decay modes have been done. New experiments are proposed. As the most favourable case, we consider the neutral currents investigation via the $^{15}N(\mathbf{p}, \alpha)^{12}C$ resonance reaction that populates the 13 MeV, $J^\pi = 2^\pm$ isovector parity mixed doublet. The energy anomalies for the expected interference effects, relevant for the experiments, have been found to be

$A_L = 1.4 \cdot 10^{-5}$ and $A_b = 1.4 \cdot 10^{-5}$ at $\theta = 150°$ and are based on the conservative value of 0.1 eV for the PNC matrix element. Such an experiment together with the PNC α-decay experiment (an isoscalar case) [45] would fix from the experiment the isoscalar and isovector strengths of the H_{PNC}-interaction.

We reexamined estimates of the circular polarization of γ rays emitted in the transition $\frac{1^-}{2}$, $T = \frac{1}{2}$ (2.789 MeV) $\rightarrow \frac{3^+}{2}$, $T = \frac{1}{2}$ (g.s.) in ^{21}Ne, which involves the parity admixture of two closed states $\frac{1^-}{2}$, $T = \frac{1}{2}$ (2.789 MeV) and $\frac{1^+}{2}$, $T = \frac{1}{2}$ (2.796 MeV). New estimates have been added to previous ones. From the study a different interpretation of the measurement is suggested. Contrarily to the previous claim by Brandenburg et al. [28], we found that the isovector contribution is well defined in sign, while the isoscalar contribution is not and somewhat disfavoured. This conclusion agrees with the recent result of Ref. [43] based on much larger valence basis. Unfortunately a more precise experiment using the Compton polarimeters compared to those already done [16] at present is impossible to perform.

ACKNOWLEDGEMENTS

The author would like to thank Professor Luciano Fonda for his permanent encouragement, Professor B.Desplanques and P.G.Bizzeti and G.Clausnitzer for fruitful discussions during his visits at the Univerity of Florence, University of Giessen and Institute for Nuclear Sciences from Grenoble, respectively, Professor B.Alex Brown for providing the OXBASH code and interesting discussions, Dr. M.Horoi for many years of collaboration. He would also like to thank Professor Abdus Salam, the International Atomic Energy Agency and UNESCO for hospitality at the International Centre for Theoretical Physics, Trieste.

REFERENCES

1. **Bludman S.A.** — Nuovo Cimento, G, 1958, p.433.
2. **Glashow S.L.** — Nucl. Phys., 1961, vol.22, p.579.
3. **Salam A., Ward J.C.** — 1964, vol.13, p.168.
4. **Weinberg S.** — Phys. Rev. Lett., 1967, vol.19, p.1264.
5. **Higgs P.W.** — Phys. Rev. Lett., 1964, vol.13, p.508.
6. **Englert F., Brout R.** — Phys. Rev. Lett., 1964, vol.13, p.321.
7. **Salam A.** — In: «Elementary Particle Theory», ed.N.Svartholm, Stockholm, Almqvist and Wiskel, 1968, p.367.

8. **Hasert F.J. et al.** — Phys. Rev. Lett., 1973, vol.46B, p.138.
9. **Arnison G. et al.** — UA-1 Collaboration, Phys. Lett., 1983, vol.122B, p.103.
10. **Banner M. et al.** — UA-2 Collaboration, 1983, vol.122B, p.476.
11. **Glashow S.L., Iliopoulos G., Maiani L.** — Phys. Rev., 1970, vol.D2, p.1285.
12. **Kobayashi M., Maskawa T.** — Prog. Theor. Phys., 1973, vol.49, p.652.
13. **Desplanques B., Donoghue J.F., Holstein B.R.** — Ann. Phys. (N.Y.), 1980, vol.124, p.449.
14. **Dubovik V.M., Zenkin S.V.** — Ann. Phys. (N.Y.), 1986, vol.172, p.100;
Dubovik V.M., Zenkin S.V., Obuchovskii I.T., Tosunyan L.A. — Fiz. Elem. Chastitz At. Yadra, 1987, vol.18, p.575; Sov. J. Part. Nucl., 1987, vol.18, p.244.
15. **Kaiser N., Meissner U.G.** — Nucl. Phys., 1988, vol.A489, p.671; 1989, vol.A499, p.699; 1990, vol.A510, p.759; Modern Physics Letters, 1990, vol.A5, No.22, p.1703.
16. **Adelberger E.G., Haxton W.C.** — Ann. Rev. Nucl. Part. Sci., 1985, vol.35, p.501.
17. **Bizzeti P.G.** — Weak Interactions in Nuclei, Riv. del Nuovo Cimento, 1983, vol.6, Nr.12, p.1.
18. **Adelberger E.G. et al.** — Phys. Rev., 1983, vol.C27, p.2833.
19. **Elsener K. et al.** — Phys. Letters, 1982, vol.B117, p.167; Phys. Rev. Letters, 1984, vol.52, p.1476.
20. **Popescu S., Dumitrescu O., Vary J.P.** — Search for Neutral Currents in ^{16}O. To be published in «Phys. Rev. C».
21. **Bunakov V.E.** — Fiz. Elem. Chastitz At. Yadra, 1995, vol.26, p.285 (Phys. Part. Nucl., 1995, vol.26, p.115).
22. **Dumitrescu O.** — «Neutral Currents in Low Energy Nuclear Physics Processes». Preprint ICTP Trieste IC/95/139, 1995, sent for publ. in Fiz. Elem. Chastitz At. Yadra.
23. **Desplanques B.** — In: «Proceedings of the VIII International Workshop on Weak Interactions and Neutrinos, Javea, 1982». Ed. A.Morales (Singapore, 1983), p.515; «Proceedings of the International Workshop on Reactors Based Fundamental Physics, Grenoble, 1983», J. Phys. (Paris), 1984, vol.45, p.55.
24. **Haxton W.C., Gibson B.F., Henley E.M.** — Phys. Rev. Lett., 1980, vol.45, p.1677.
25. **Brown B.A., Richter W.A., Godwin N.S.** — Phys. Rev. Lett., 1980, vol.45, p.1681.
26. **Snover K.A. et al.** — Phys. Rev. Lett., 1978, vol.41, p.145;
Earle E.D. et al. — Nucl. Phys., 1983, vol.A396, p.221c.
27. **Millener D.J. et al.** — Phys. Rev., 1978, vol.C18, p.1878.
28. **Brandenburg R.A. et al.** — Phys. Rev. Lett., 1978, vol.41, p.618.
29. **Desplanques B., Dumitrescu O.** — Nucl. Phys., 1993, vol.A565, p.818.
30. **Dumitrescu O., Clausnitzer G.** — Nucl. Phys., 1993, vol.A552, p.306.
31. **Kniest N. et al.** — Phys. Rev., 1990, vol.C41, p.1337.
32. **Kniest N. et al.** — Phys. Rev., 1983, vol.C27, p.906.
33. **Ohlert J., Traudt O., Waeffler H.** — Phys. Rev. Lett., 1981, vol.47, p.475.
34. **Kniest N. et al.** — Phys. Rev., 1991, vol.C44, p.491.
35. **Dumitrescu O.** — Nuclear Physics, 1991, vol.A535, p.94.
36. **Redder A. et al.** — Z. Phys., 1982, vol.A305, p.325.
37. **Dumitrescu O., Horoi M., Carstoiu F., Stratan Gh.** — Phys. Rev., 1990, vol.C41, p.1462.
38. **Preiss M. et al.** — Proc. Salzburg Meeting on Nuclear Physics, 1992. «A New Parity Mixing Doublet».

39. **Horoi M., Clausnitzer G., Brown B.A., Warburton E.K.** — Phys. Rev., 1994, vol.C50, p.775.
40. **Brandus I. et al.** — Rev. Roum. Phys., 1991, vol.36, p.135.
41. **Mihailescu D., Dumitrescu O.** — Romanian Reports in Physics, 1993, vol.45, p.661.
42. **Mihailescu D., Comisel H., Dumitrescu O.** — Romanian J. Phys., 1993, vol.39, p.223.
43. **Horoi M., Clausnitzer G., Brown B.A., Warburton E.K.** — NATO-ASI Series B: Physics, 1994, vol.334; Eds. W.Scheid and A.Sandulescu (Plenum Press, N.Y.—London); **Horoi M., Brown B.A.** — Phys. Lett., 1995, vol.74, p.231.
44. **Carstoiu F., Dumitrescu O., Stratan G., Braic M.** — Nucl. Phys., 1985, vol.A441, p.221.
45. **Neuebeck K., Schober H., Waeffler H.** — Phys. Rev., 1974, vol.C10, p.320.
46. **Dumitrescu O., Stratan G.** — Nuovo Cimento, 1991, vol.105A, p.901.
47. **Horoi M.** — Phys. Rev., 1994, vol.C50, p.2392.
48. **Frankle C.M. et al.** — Phys. Rev., 1992, vol.C46, p.778.
49. **Barnes C.A. et al.** — Phys. Rev. Lett., 1979, vol.40, p.840.
50. **Mak H.B. et al.** — Reports on Research in Nuclear Physics at Queens University (Kingston, Ont., 1981), p.19.
51. **Bini M., Fazzini T.F., Poggi G., Taccetti N.** — Phys. Rev., 1988, vol.C38, p.1195; Phys. Rev. Lett., 1985, vol.55, p.795.
52. **Bizzeti P.G. et al.** — Lett. Nuovo Cimento, 1980, vol.29, p.167;
Mauzenzig P.R. et al. — In: «Proceedings of the 1979 International Conf. on Neutrinos, Weak Interactions and Cosmology». Vol.2, Eds. A.Haatuft and C.Jarlskog (Bergen, 1979), p.97;
Bini M., Bizzeti P.G., Sona P. — Phys. Rev., 1981, vol.C23, p.1265; Lett. Nuovo Cimento, 1984, vol.41, p.191.
53. **Afrens G. et al.** — Nucl. Phys., 1982, vol.A390, p.486.
54. **Bizzeti P.G.** — Phys. Rev., 1986, vol.C33, p.1837.
55. **Adelberger E.G., Hoodbhoy P., Brown B.A.** — Phys. Rev., 1984, vol.C30, p.456; 1986, vol.C33, p.1840.
56. **Zeps V.J., Thesis Ph.D.** — University of Washington, 1989;
Zeps V.J. et al. — A.I.P. Conf. Proceedings, 1989, vol.176, p.1098;
Swanson H.E. et al. — Heidelberg Conf. Proc., 1986, p.648 and p.277. Weak and Electromagnetic Interactions in Nuclei. Eds. H.V.Klapdoor and J.Metzinger.
57. **Bini M., Bizzeti P.G., Sona P.** — Phys. Rev., 1980, vol.C23, p.1265.
58. **Karlsen R.E.** — Europhys. Lett., 1993, vol.22(2), p.341.
59. **Henley E.M., Hwang W.-Y.P., Kisslinger L.S.** — To be published in Physics Letters.
60. **Henley E.M., Pasupathy J.** — Nucl. Phys., 1993, vol.A556, p.467;
Henley E.M., Hwang W.-Y.P., Kisslinger L.S. — Phys. Rev., 1992, vol.D46, p.431;
Hatsuda T. et al. — Phys. Rev., 1993, vol.C49, p.452;
Reinders L.J., Rubinstein H., Yazaki S. — Nucl. Phys., 1983, vol.B213, p.109.
61. **Grach I., Shmatikov.** — ITEP Preprint 100–88, 1988.
62. **Khatsimovskii V.M.** — Preprint 84-164; Inst. Nucl. Phys. Novosibirsk; Yad. Fiz. (USSR), 1985, vol.42, p.1236; Sov. J. Nucl. Phys., 1985, vol.42(5), p.781.
63. **Brown B.A., Etchegoyen A., Rae W.D.M.** — MSU–NSCL Report, 1985, vol.524;
Brown B.A. et al. — MSU–NSLL Report, Michigan State University version of the OXBASH code, 1988, vol.524;
Brown B.A., Wildenthal B.H. — Annu. Rev. Nucl. Part. Sci., 1988, vol.38, p.29.

64. **Ajzenberg F.** — Selove Nucl. Phys., 1987, vol.A499, 1 (A = 13–15); 1987, vol.A475, 1, (A = 18–20); 1986, vol.A460, 1, (A = 16, 17); 1985, vol.A433, 1, (A = = 11, 12); 1979, vol.A320, 1, (A = 5–10); 1977, vol.A281, 1, (A = 16, 17).
65. **Miller G.A., Spenser J.E.** — Ann. Phys. (N.Y.), 1976, vol.100, p.562.
66. **Dumitrescu O., Gari M., Kuemmel H., Zabolitzky J.G.** — Zeit. Naturforschung, 1972, vol.A27, p.733; Phys. Lett., 1971, vol.35B, p.19.
67. **Gari M.** — Physics Reports, 1973, vol.C6, p.317.
68. **Machleidt R., Holinde K., Elster Ch.** — Physics Reports, 1987, vol.149, p.1; **Machleidt R.** — Adv. Nucl. Phys., 1989, vol.19, p.189.
69. **Lacomb M. et al.** — Phys. Rev., 1980, vol.C21, p.861.
70. **Gari M.F., Kruempelmann W.** — Z. Phys., 1985, vol.A322, p.689; **Gari M.F., Kruempelmann W.** — Phys. Lett., 1986, vol.B173, p.10; **Deister S., Gari M.F., Kruempelmann W., Mahlke M.** — Few-Body Systems, 1991, vol.10, p.1.
71. **Kuo T.T.S., Brown G.E.** — Nucl. Phys., 1966, vol.85, p.40.
72. **Kuo T.T.S.** — Ann. Rev. Nucl. Part. Sci., 1974, vol.24, p.101; Nucl. Phys., 1967, vol.A103, p.71.
73. **Dumitrescu O.** — «Parity Nonconservation in Nuclear Reactions and Alpha Decay», Proc. Predeal Summer School «Recent Advances in Nuclear Structure» 28 Aug. — 8 Sept., 1990; Eds. D.Bucurescu, G.Cata — Danil and N.V.Zamfir, World Scientific, Singapore — New Jersey — London — Hong Kong, 1991, p.359.
74. **Day B.D.** — Rev. Mod. Phys., 1967, vol.39, p.719; 1978, vol.50, p.495.
75. **Rajaraman R., Bethe H.A.** — Rev. Mod. Phys., 1967, vol.39, p.745.
76. **Zuker A.P., Buck B., McGrory J.B.** — Phys. Rev. Lett., 1968, vol.21, p.39.
77. **Zuker A.P.** — Phys. Rev. Lett., 1969, vol.23, p.983.
78. **Reehal B.S., Wildenthal B.H.** — Part. and Nucl., 1973, vol.6, p.137.
79. **Tanner N.** — Phys. Rev., 1957, vol.107, p.1203.
80. **Feynman R.P., Gell-Mann M.** — Phys. Rev., 1958, vol.109, p.193.
81. **Lobashov V.M. et al.** — JETP Lett., 1967, vol.5, p.59; Phys. Lett., 1967, vol.25, p.104.
82. **Barton G.** — Nuovo Cimento, 1961, vol.19, p.512.
83. **Skyrme T.H.R.** — Proc. Roy. Soc., 1961, vol.A260, p.127.
84. **Witten E.** — Nucl. Phys., 1983, vol.B223, p.422,433.
85. **Meissner Ulf-G.** — Physics Reports, 1988, vol.161, p.213.
86. **Zahed I., Brown G.E.** — Physics Reports, 1986, vol.142, p.1.
87. **Schwesinger B., Weigel H., Holzwarth G., Hayashi A.** — Physics Reports, 1989, vol.173, p.173.
88. **Meissner Ulf-G., Zahed I.** — Adv. Nucl. Phys., 1986, vol.17, p.143.
89. **Holzwarth G., Schwesinger B.** — Rep. Prog. Phys., 1986, vol.49, p.825.
90. **Bethe H.A.** — Ann. Rev. Nucl. Sci., 1971, vol.21, p.93.
91. **Feenberg E.** — Theory of Quantum Fluids. 1969, New York, Academic Press.
92. **Cummings E.D., Bucksbaum P.H.** — Weak Interactions of Leptons and Hadrons. Cambridge University Press, 1983.
93. **Donoghue J.F., Golowich E., Holstein B.R.** — Physics Reports, 1980, vol.131, p.319, No.5 and 6.
94. **Henley E.M.** — Phys. Lett., 1968, vol.B28, p.1; Ann. Rev. Nucl. Sci., 1969, vol.19, p.367.

95. **Holstein B.R.** — Weak Interactions in Nuclei. Princeton series in Physics, 1989.
96. **Caprini I. and Micu L.** — Phys. Rev., 1988, vol.C37, p.2209; Phys. Lett., 1985, vol.B153, p.8.
97. **Itzykson C., Zuber J.B.** — Quantum Field Theory. McGraw–Hill, New York, 1980.
98. **Walecka D.** — Ann. Phys. (N.Y.), 1974, vol.83, p.491;
Serot B.D. — Nucl. Phys., 1983, vol.A446, p.97c.
99. **Kuemmel H.** — Nucl. Phys., 1971, vol.A146, p.205.
100. **Kuemmel H., Luermann K.H., Zabolitzky J.G.** — Phys. Rep., 1978, vol.36, p.1
101. **Irvine J.M.** — Rep. Progr. Phys., 1988, vol.51, p.1181.
102. **Kallio A., Day B.D.** — Phys. Lett., 1967, vol.B25, p.72; Nucl. Phys., 1968, vol.A124, p.177.
103. **Reid R.V. Jr.** — Annals Phys. (N.Y.), 1968, vol.50, p.411.
104. **Reehal B.S., Wildenthal B.H.** — Part. Nucl., 1973, vol.6, p.137.
105. **Cohen S., Kurath D.** — Nucl. Phys., 1965, vol.A73, p.1.
106. **Preedom O., Wildenthal B.H.** — Phys. Rev., 1972, vol.C6, p.1633.
107. **Millener D.J., Kurath D.** — Nucl. Phys. 1975, vol.A255, p.315.
108. **Wilkinson J.H.** — The Algebraic Eigenvalue Problem. Clarendon Press, Oxford, 1965.
109. **Whitehead R.R.** — In: «Moment Methods in Many Fermion Systems». Ed. B.J.Dalton, S.M.Grimes, J.P.Vary, S.A.Wiliams. Plenum Press, New York, 1980, p.235.
110. **Horoi M., Brown B.A., Zelevinsky V.** — Phys. Rev., 1994, vol.C50, p.R2274.
111. **Brown B.A., Rahdi R., Wildenthal B.H.** — Phys. Rep., 1983, vol.101, p.313.
112. **McGrory J.B., Wildenthal B.H.** — Phys. Rev., 1973, vol.C7, p.654; Ann. Rev. Nucl. Sci., 1980, vol.30, p.383.
113. **Brown B.A., Wildenthal B.H.** — Ann. Rev. Nucl. Part. Sci., 1988, vol.38, p.29; Phys. Lett., 1987, vol.198B, p.29; Phys. Rev., 1983, vol.C27, p.1296.
114. **Wildenthal B.H.** — Progr. Part. Nucl. Phys., 1984, vol.11, p.5. Ed. by D.H.Wikinson, Pergamon — Oxford. Phys. Rev. Lett., 1974, vol.33, p.233.
115. **Seth K.K. et al.** — Phys. Rev. Lett., 1974, vol.33, p.233.
116. **Federman P., Pittel S.** — Phys. Rev., 1969, vol.186, p.1106.
117. **Brown B.A. et al.** — Ann. Phys. (N.Y.), 1988, vol.182, p.191.
118. **Gloekner D.H., Lawson D.R.** — Phys. Lett., 1974, vol.53B, p.313.
119. **Soloviev V.G.** — Theory of Complex Nuclei. Nauka, Moscow, 1971; Pergamon Press, New York, 1976.
120. **Mahaux C., Weidenmueller H.A.** — Shell Model Approach to Nuclear Reactions. North-Holland, Amsterdam, 1969.
121. **Preiss M., Clausnitzer G.** — NATO ASI Series B: Physics, 1994, vol.334, p.353.
122. **Biesiot W., Smith Ph.B.** — Phys. Rev., 1981, vol.C24, p.2443.
123. **Bizzeti P.G., Maurenzig P.R.** — Nuovo Cimento, 1980, vol.A56, p.492.
124. **Krane K.S., Olsen C.E., Sites J.R., Steyert W.A.** — Phys. Rev., 1971, vol.C4, p.1906.
125. **Dahlinger M. et al.** — Nucl. Phys., 1988, vol.A484, p.337.
126. **Pepper G.H., Brown L.** — Nucl. Phys., 1976, vol.A260, p.163;
Bray K.H., Frawley A.D., Opfel T.R., Barker F.R. — Nucl. Phys., 1977, vol.A288, p.334.
127. **Haxton W.C.** — Private Communication.

128. **Haxton W.C.** — Proc. Symp./Workshop Spin Symm., Triumf, Vancouver June 30—July 2, 1989; Eds. W.D.Ramsay and W.T.H. van Oers, 1989, p.13.
129. **Wagner G.J. et al.** — Phys. Rev., 1977, vol.C16, p.1271.
130. **Leavit R.A. et al.** — Nucl. Phys., 1983, vol.A410, p.83.
131. **Browne E.** — Nuclear Data Sheets, 1987, vol.52, p.127.
132. **Endt D.M.** — Nucl. Phys., 1990, vol.A521, p.1.
133. **Blin-Stoyle R.J.** — Fundamental Interactions and the Nucleus, North-Holland, Amsterdam, 1973.
134. **Bohr A., Mottelson B.** — Nuclear Structure. Benjamin, N.Y., 1975.
135. **Gari M., McGrory J.B., Offerman R.** — Phys. Lett., 1975, vol.B55, p.277.
136. **Michel F.C.** — Phys. Rev., 1964, vol.B133, p.329.
137. **Desplanques B., Missimer J.** — Nucl. Phys., 1978, vol.A300, p.286; **Desplanques B.** — Nucl. Phys., 1975, vol.A242, p.423.
138. **Desplanques B.** — Nucl. Phys., 1979, vol.A316, p.244.
139. **Chemtob M., Desplanques B.** — Nucl. Phys., 1974, vol.B78, p.139.
140. **Gari M., Reid J.H.** — Phys. Lett., 1974, vol.53B, p.237.
141. **Desplanques B. et al.** — Z. Phys. C – Particles and Fields, 1991, vol.51, p.499; **Bernabeu J. et al.** — Z. Phys. C – Particles and Fields, 1990, vol.46, p.323.
142. **Desplanques B.** — Nucl. Phys., 1980, vol.A335, p.147.
143. **Brown B.A., Wildenthal B.H.** — Annu. Rev. Nucl. Part. Sci., 1988, vol.38, p.29.
144. **Warburton E.K., Becker J.A., Brown B.A.** — Phys. Rev., 1990, vol.C41, p.1147.
145. **Brown B.A., Wildenthal B.H.** — At. Data and Nucl. Data Table, 1985, vol.33.
146. **Spits A.M., Kopecky J.** — Nucl. Phys., 1990, vol.A521, p.1.